# Identification of Novel β-Tubulin Inhibitors Using a Combined *In Silico*/*In Vitro* Approach

*Mark James Horgan[1], Lukas Zell[2] , Bianka Siewert[1], Hermann Stuppner[1], Daniela Schuster[2] and *Veronika Temml[2]*

[1]Institute of Pharmacy/Pharmacognosy, Center for Chemistry and Biomedicine, University of Innsbruck, Innrain 80-82, 6020 Innsbruck, Austria. [2]Institute of Pharmacy, Department of Pharmaceutical and Medicinal Chemistry, Paracelsus Medical University Salzburg, Strubergasse 21, 5020 Salzburg, Austria.

*E-mail: veronika.temml@pmu.ac.at

## Supporting Information

1. Actives dataset generation

**Table S1.** List of ligands active against tubulin used to generate the actives dataset for pharmacophore model training.

| ID | Name | Tubulin activity | SMILES | Reference |
|---|---|---|---|---|
| **AS1** | Thiabendazole | 81.6 ± 1% inhibition at 20 μM | C1=CC=C2C(=C1)NC(=N2)C3=CSC=N3 | [1] |
| **AS2** | Albendazole | $IC_{50}$ = 6.9 μM | CCCSC1=CC2=C(C=C1)N=C(N2)NC(=O)OC | [2] |

| | | | | |
|---|---|---|---|---|
| **AS3** | Fenbendazole | $IC_{50}$ = 5.4 µM | COC(=O)Nc1nc2ccc(Sc3ccccc3)cc2[nH]1 | [2] |
| **AS7** | Mebendazole | $IC_{50}$ = 6.1 µM | COC(=O)NC1=NC2=C(N1)C=C(C=C2)C(=O)C3=CC=CC=C3 | [2] |
| **AS8** | Flubendazol | $IC_{50}$ = 3.5 µM | COC(=O)Nc1nc2cc(C(=O)c3ccc(F)cc3)ccc2[nH]1 | [2] |
| **AS9** | Parbendazol | $IC_{50}$ = 3.1 µM | CCCCc1ccc2[nH]c(NC(=O)OC)nc2c1 | [2] |
| **AS10** | Oxfendazole | $IB_{50}$ = 1.3 µM (Mebendazole inhibitory binding) | COC(=O)NC1=NC2=C(N1)C=C(C=C2)S(=O)C3=CC=CC=C3 | [3] |
| **AS11** | Oxibendazole | $IC_{50}$ = 2.4 µM | CCCOc1ccc2[nH]c(NC(=O)OC)nc2c1 | [2] |
| **AS5** | Nocodazole | $IC_{50}$ = 1.82 ± 0.06µM | COC(=O)NC1=NC2=C(N1)C=C(C=C2)C(=O)C3=CC=CS3 | [4] |
| **AS12** | CHEMBL459773 | $IC_{50}$ = 4.23 µM | COC1=C(OC)C(OC)=CC(C(C2=CSC(C3=CC=CC=C3)=N2)=O)=C1 | [5] |
| **AS13** | CHEMBL3426932 | $IC_{50}$ = 2.36 µM | COC1=C(OC)C(OC)=CC(C2=C(C3=CC=C(OCC)C=C3)N=C(N)S2)=C1 | [6] |
| **AS14** | CHEMBL273081 | $IC_{50}$ = 16.75 µM | ClC1=C(/N=C2S/C(C(N/2)=O)=C/C3=CC=C(N(C)C)C=C3)C=CC=C1 | [7] |
| **AS15** | 24045-22-5 | $IC_{50}$ = 4.0 ± 0.6 µM | O=C(N/1)/C(SC1=N\C2=CC=C(O)C=C2)=C\C3=CC(OC)=C(O)C=C3 | [8] |
| **AS16** | 1596344-07-8 | $IC_{50}$ = 5.6 ± 0.3 µM | O=C(N/1)/C(SC1=N\C2=CC=C(OC3=CC=CC=C3)C=C2)=C\C4=C(O)C=CC=C4 | [8] |
| **AS17** | 463979-31-9 | $IC_{50}$ = 6.28 µM | O=C(N/1)/C(SC1=N\C2=CC=C(O)C=C2)=C\C3=CC(OC)=CC=C3 | [9] |
| **AS4** | 356542-94-4 | $IC_{50}$ = 1.5 µM | O=C(C1=CC(OC)=C(O)C=C1)/C=C/C2=C(OC)C=C(OC)C=C2OC | [10,11] |
| **AS18** | CHEMBL1163178 | $IC_{50}$ = 6.8 ± 0.6 µM | O=C(C1=CC=C(Cl)C=C1)CC(SC(N(CC)CC)=S)C2=CC=CC=C2 | [12] |
| **AS19** | CHEMBL220818 | $IC_{50}$ = 2.2 µM | O=C(C1=CC(OC)=C(OC)C(OC)=C1)/C=C/C2=CC=C(C=CC=C3)C3=C2 | [13] |
| **AS20** | CHEMBL285901 | $IC_{50}$ = 2.8 µM | O=C(C1=CC(OC)=C(OC)C(OC)=C1)/C=C/C2=CC=C(N(C)C)C=C2 | [13] |
| **AS21** | 1585234-76-9 | $IC_{50}$ = 1.6 ± 0.32 µM | COC1=C(C(OC)=CC(OC)=C1)/C=C/C(C2=CC(N)=CC=C2)=N\O | [14] |
| **AS22** | CHEMBL3393090 | $IC_{50}$ = 1.3 ± 0.0 µM | OC1=CC(/C=C/C(C2=CC=CC=C2C3=CC=C(F)C=C3)=O)=CC=C1OC | [15] |
| **AS23** | CHEMBL3393091 | $IC_{50}$ = 3.4 ± 0.2 µM | FC(C=C1)=CC=C1C2=CC=CC=C2C(/C=C/C3=CC=C(OC)C(B(O)O)=C3)=O | [15] |
| **AS24** | CHEMBL3393092 | $IC_{50}$ = 3.6 ± 0.0 µM | FC(C=C1)=CC=C1C2=CC=CC=C2C(/C=C/C3=CC=C(N(C)C)C=C3)=O | [15] |
| **AS25** | CHEMBL3393099 | $IC_{50}$ = 0.49 ± 0.27 µM | FC1=CC=CC(C2=CC=CC=C2C(/C=C/C3=CC=C(C(O)=C3)OC)=O)=C1 | [15] |
| **AS26** | CHEMBL3818930 | $IC_{50}$ = 1.99 ± 0.03 µM | O=C(/C(CC1=C2OC)=C/C3=C4C=CNC4=CC=C3)C1=CC(OC)=C2OC | [16] |
| **AS27** | CHEMBL3818850 | $IC_{50}$ = 2.68 ± 0.15 µM | O=C(C1=CC(OC)=C(OC)C(OC)=C1)/C(C)=C/C2=CNC3=C2C=CC(OC)=C3 | [17] |

| | | | | |
|---|---|---|---|---|
| **AS28** | CHEMBL595808 | $IC_{50}$ = 12 µM | COC1=C(OC)C(OC)=CC(C(/C=C/C2=C(OC)C=C(OC)C=C2OC)=O)=C1 | [18] |
| **AS29** | CHEMBL9859 | $IC_{50}$ = 0.46 µM | COC1=C(OC)C(OC)=CC(C(/C(C)=C/C2=CC=C(OC)C(O)=C2)=O)=C1 | [19] |
| **AS30** | CHEMBL107 | $IC_{50}$ = 6.7 ± 0.05 µM | CC(=O)N[C@H]1CCC2=CC(=C(C(=C2C3=CC=C(C(=O)C=C13)OC)OC)OC)OC | [20] |
| **AS31** | CHEMBL208189 | $IC_{50}$ = 8.3 µM | CC(=O)CN[C@H]1CCC2=CC(=C(C(=C2C3=CC=C(C(=O)C=C13)OC)OC)OC)OC | [21] |
| **AS32** | CHEMBL206877 | $IC_{50}$ = 4.6± 0.17 µM | COC1=CC=C2C(=CC1=O)[C@H](CCC3=CC(=C(C(=C32)OC)OC)OC)NC4=C(C=C(C=C4)[N+](=O)[O-])[N+](=O)[O-] | [21] |
| **AS33** | CHEMBL2180999 | $IC_{50}$ = 1.62 µM | COC1=CC=C2C(=CC1=O)[C@H](CCC3=CC(=C(C(=C32)OC)OC)OC)NCC4=C(C(=CC=C4)F)F | [22] |
| **AS34** | CHEMBL4553296 | $IC_{50}$ = 0.05 µM | O(C)C1=C2C=3C([C@@H](NC(C)=O)CCC2=CC(OC)=C1OC)=CC(=O)C(NC4=CC(C(F)(F)F)=C(Cl)C=C4)=CC3 | [23] |
| **AS35** | CHEMBL1946973 | $IC_{50}$ = 1.1 ± 0.1 µM | COC1=C(OC)C(OC)=CC(N2C(C3=CC=C(OCC)C=C3)=NN=N2)=C1 | [24] |
| **AS36** | CHEMBL1823147 | $IC_{50}$ = 3.0 ± 0.6 µM | COC1=C(OC)C(OC)=CC(C(C2=C(C)OC3=C(O)C(OC)=CC=C23)=O)=C1 | [25] |
| **AS37** | CHEMBL3580699 | $IC_{50}$ = 14 ± 2.2 µM | COC1=C(OC)C(OC)=CC(C2=C(NC3=CC=C(OC)C=C3)N(C=CC=C4)C4=N2)=C1 | [26] |
| **AS38** | 7-Methoxy-4-(3,4,5-trimethoxyphenyl)quinolin-2(1H)-one | $IC_{50}$ = 2.56 ± 0.15 µM | COC1=C(OC)C(OC)=CC(C(C2=CC=C(CC)C=C2N3)=CC3=O)=C1 | [27] |
| **AS39** | CHEMBL221765 | $IC_{50}$ = 2.0 µM | COC1=CC(SC2=C(C(OC)=O)NC3=CC=C(OC)C=C23)=CC(OC)=C1OC | [28] |
| **AS40** | CHEMBL380871 | $IC_{50}$ = 4.5 ± 0.1 µM | COC1=CC(SC2=C(C(OC)=O)NC3=CC=C([N+]([O-])=O)C=C23)=CC(OC)=C1OC | [29] |
| **AS41** | 1179587-98-4 | IC50 = 1.3 ± 0.1 µM | COC1=CC(SC2=C(C(OC)=O)NC3=CC=C(Br)C=C23)=CC(OC)=C1OC | [30] |
| **AS42** | 1179588-09-0 | $IC_{50}$ = 0.67 ± 0.02 µM | COC1=CC(C(C2=C(C(OC)=O)NC3=CC=C(OC)C=C23)=O)=CC(OC)=C1OC | [30] |
| **AS43** | 1839121-23-1 | $IC_{50}$ = 8.3 µM | O=C(C(NC1=CC=C(OC)N=C1)=O)C2=CN(CC3OCCC3)C4=C2C=CC=C4 | [31] |
| **AS44** | CHEMBL3747333 | $IC_{50}$ = 6.6 µM | O=C(C(NC1=CC=C(OC(C)C)N=C1)=O)C2=CN(CCOC)C3=C2C=CC=C3 | [31] |
| **AS45** | 1582297-75-3 | $IC_{50}$ = 1.65 µM | CC1=C([Se](C2=CC(OC)=C(OC)C(OC)=C2)=O)C3=C(N1)C=CC=C3 | [32] |
| **AS46** | CHEMBL4092940 | $IC_{50}$ = 11.2 ± 1.13 µM | ClC1=CC(NC(C(C2=CC=CS2)=O)=C3NC4=C([N+]([O-])=O)C=NC(N5CCN(C)CC5)=N4)=C3C=C1 | [33] |
| **AS47** | CHEMBL1940254 | $IC_{50}$ = 1.1 ± 0.5 µM | COC1=CC(SC2=C(C3=CC=CN3)NC4=CC=CC=C24)=CC(OC)=C1OC | [34] |

| | | | | |
|---|---|---|---|---|
| **AS48** | CHEMBL1940258 | $IC_{50}$ = 0.74 ± 0.05 µM | COC1=CC(SC2=C(C3=CC=CS3)NC4=CC=CC=C24)=CC(OC)=C1OC | [34] |
| **AS49** | CHEMBL2313790 | $IC_{50}$ = 1.3 ± 0.06 µM | COC1=CC(SC2=C(N3C=CN=C3)NC4=CC=CC=C24)=CC(OC)=C1OC | [35] |
| **AS50** | CHEMBL3597212 | $IC_{50}$ = 1.1 ± 0.1 µM | COC1=CC(SC2=C(C3=CC=CC=C3)NC4=CC(OC)=CC=C24)=CC(OC)=C1OC | [36] |
| **AS51** | CHEMBL3597223 | $IC_{50}$ = 1.2 ± 0.1 µM | COC1=CC(=CC(=C1OC)OC)SC2=C(NC3=C2C=CC(=C3Cl)Cl)C4=CC=CC=C4 | [36] |
| **AS52** | CHEMBL89341 | $IC_{50}$ = 1.1 ± 0.4 µM | COC1=CC(C(C2=C(C3=CC(O)=C(OC)C=C3)NC4=CC(OC)=CC=C24)=O)=CC(OC)=C1OC | [37] |
| **AS53** | CHEMBL2442345 | $IC_{50}$ = 1.1 ± 0.4 µM | COC1=CC(C(C2=C(C3=CC(O)=C(OC)C=C3)NC4=C(OC)C(OC)=CC=C24)=O)=CC(OC)=C1OC | [37] |
| **AS54** | CHEMBL20684 | $IC_{50}$ = 2.2 µM | COC1=CC=C(S(NC2=CC=CN=C2NC3=CC=C(O)C=C3)(=O)=O)C=C1 | [38] |
| **AS55** | CHEMBL281995 | $IC_{50}$ = 2.1 µM | COC1=CC=C(S(NC2=C3C(C=C(Cl)N3)=CC=C2)(=O)=O)C=C1 | [38] |
| **AS56** | CHEMBL20289 | $IC_{50}$ = 9.5 µM | COC1=CC=C(S(NC2=C3C(C(Cl)=CN3)=CC=C2)(=O)=O)C=C1 | [38] |
| **AS57** | CHEMBL20296 | $IC_{50}$ = 88.5 µM | ClC1=CC=C(S(NC2=C3C(C=C(Cl)N3)=CC=C2)(=O)=O)C=C1 | [39] |
| **AS58** | CHEMBL20800 | $IC_{50}$ = 2.9 µM | CC1=CC=C(C=C1)S(=O)(=O)NC2=CC=CC3=C2NC(=C3)O | [39] |
| **AS59** | SCHEMBL3072090 | $IC_{50}$ = 2.5 µM | CC1=CC=C(S(NC2=C3C(CC(N3)=O)=CC=C2)(=O)=O)C=C1 | [40] |
| **AS60** | CHEMBL216379 | $IC_{50}$ = 1.1 ± 0.1 µM | O=C(NC1=C2C(CCN2S(C3=CC=C(OC)C=C3)(=O)=O)=CC=C1)C4=CC=NC=C4 | [41] |
| **AS61** | CHEMBL216327 | $IC_{50}$ = 1.2 ± 0.1 µM | O=C(NC1=C2C(CCN2S(C3=CC=C(OC)C=C3)(=O)=O)=CC=C1)C4=CC=CO4 | [41] |
| **AS62** | CHEMBL230296 | $IC_{50}$ = 0.6 µM | COC1=NC(OC)=C(NS(C2=CC3=C(N(C)C4=C3C=CC=C4)C=C2)(=O)=O)C=C1 | [42] |
| **AS63** | CHEMBL79280 (Betabulin) | $IC_{50}$ = 2 µM | COC1=C(F)C=C(NS(C2=C(F)C(F)=C(F)C(F)=C2F)(=O)=O)C=C1 | [43] |
| **AS64** | CHEMBL2397992 | $IC_{50}$ = 3.68 µM | COC1=CC(OC)=CC(OC)=C1/C=C/S(NC2=CC=C(OC)C(N)=C2)(=O)=O | [44] |
| **AS65** | CHEMBL141689 | $IC_{50}$ = 3.6 µM | COC1=CC=C(CNC2=NC(NCC3=CC=C(OC)C=C3)=C4C(N(C(C)C)C=N4)=N2)C=C1 | [45] |
| **AS66** | CHEMBL2001473 | Tubulin polymerization MIC = 20 µM | COC1=CC=C(CNC2=NC(NCC3=CC=C(OC)C=C3)=NC(NC4CCCCC4)=N2)C=C1 | [46] |
| **AS67** | CHEMBL1968484 | Tubulin polymerization MIC = 10 µM | COC1=CC=C(CNC2=NC(NCC3=CC=C(OC)C=C3)=NC(NC(C)C)=N2)C=C1 | [46] |
| **AS68** | CHEMBL1976996 | Tubulin polymerization MIC = 5 µM | COC1=C(OC)C=C(CNC2=NC(NCC3=CC=C(OC)C=C3)=NC(NC4CCCCC4)=N2)C=C1 | [46] |

| | | | | |
|---|---|---|---|---|
| **AS69** | CHEMBL141477 | $IC_{50}$ = 2 µM | COC1=CC=C(CNC2=NC(NCC3=CC=C(OC)C=C3)=C4C(N(C5CCCCC5)C=N4)=N2)C=C1 | 47 |
| **AS70** | SCHEMBL2905972 | $IC_{50}$ = 16 ± 2 µM | COC1=CC=C(CNC2=NC(NCC3=CC=C(OC)C=C3)=C4C(C(C(C)C)=NN4)=N2)C=C1 | 48 |
| **AS71** | CHEMBL513813 | $IC_{50}$ = 3.4 µM | COC1=CC=C(CNC2=NC3=CC=NN3C(NCC4=CC=C(OC)C=C4)=N2)C=C1 | 45 |
| **AS72** | CHEMBL466716 | $IC_{50}$ = 3.6 µM | COC1=CC=C(CNC2=NC3=C(C(C)C)C=NN3C(NCC4=CC=C(OC)C=C4)=N2)C=C1 | 45 |
| **AS6** | CHEMBL61 | $IC_{50}$ = 1.3 ± 0.06 µM | COC(C=C([C@H]1C2[C@H](COC2=O)[C@@H](O)C3=CC4=C(OCO4)C=C13)C=C5OC)=C5OC | 49 |
| **AS73** | CHEMBL2165487 | $IC_{50}$ = 7.7 ± 1.1 µM | COc1cc([C@@H]2c3cc4c(cc3[C@](O)(C3(O)CCCCC3)[C@H]3COC(=O)[C@H]23)OCO4)cc(OC)c1OC | 50 |
| **AS74** | CHEMBL2165463 | 21.1 % inhibition at 1 µM | COc1cc([C@@H]2c3cc4c(cc3[C@@](O)(C3(O)CCOCC3)[C@H]3COC(=O)[C@@H]23)OCO4)cc(OC)c1OC | 50 |
| **AS75** | CHEMBL2165468 | 84.5% inhibition at 1 µM (IC50 = 0.45 ± 0.05 µM) | O=C1[C@@]2([C@@H](C=3C([C@H]([C@@H](C)C)[C@]2(CO1)[H])=CC4=C(C3)OCO4)C5=CC(OC)=C(OC)C(OC)=C5)[H] | 50 |
| **AS76** | 266685-31-8 | $IC_{50}$ = 0.17 µM | COC(C=C(C1C2=C(COC2=O)NC3=CC4=C(OCO4)C=C13)C=C5OC)=C5OC | 51 |
| **AS77** | 1260403-30-2 | $IC_{50}$ = 0.27 µM | O=C1OCC2=C1C(C3=CC4=C(C=C3N2)OCO4)/C=C/C5=CC(OC)=C(OC)C(OC)=C5 | 51 |
| **AS78** | CHEMBL114642 | $IC_{50}$ = 2.3 µM | O=C1C2=C(C=CC=C2)C(C3=CC=C(OC)C(O)=C3)C4=CC=CC=C41 | 52 |
| **AS79** | CHEMBL392633 | $IC_{50}$ = 0.56 µM | COC1=CC=C(C=C1)S(=O)(=O)OC2=C3C=CC=CC3=CC4=CC=CC=C42 | 53 |
| **AS80** | CHEMBL455138 | $IC_{50}$ = 0.52 µM | O=C1C2=C(C=CC=C2)/C(C3=CC=CC=C31)=C\C(C4=CC=C(OC)C=C4)=O | 54 |
| **AS81** | CHEMBL1210677 | $IC_{50}$ = 1.5 µM | O=C1C2=C(C=CC=C2)/C(C3=CC=CC=C31)=N\OCC4=CC=C(OC)C=C4 | 55 |
| **AS82** | CHEMBL1814612 | $IC_{50}$ = 0.44 µM | O=C1C2=C(C=CC=C2)/C(C3=CC=CC=C31)=N\C4=CC=C(OC)C(O)=C4 | 56 |
| **AS83** | CHEMBL1814615 | $IC_{50}$ = 1.11 µM | O=C1C2=C(C=CC=C2Cl)/C(C3=CC=CC(Cl)=C31)=N\C4=CC=C(OC)C(O)=C4 | 56 |
| **AS84** | CHEMBL4585656 | 51.0 ± 11.2 % inhibition at 10 µM | OC1=C(C)C=C2C([C@H](C)CC/C=C(C)\C2)=C1 | 57 |
| **AS85** | CHEMBL4551469 | 56.3 ± 7.5 % inhibition at 10 µM | C[C@H]1C2=CC(OC(C3=CC=CC=C3)=O)=C(C)C=C2C/C(C)=C\CC1 | 57 |
| **AS86** | 2301070-52-8 | 58.1 ± 25.3 % inhibition at 10 µM | OC1=C(C)C=C2C([C@H](C)CCC/C(C)=C\2)=C1 | 57 |
| **AS87** | CHEMBL4590152 | 38.7 ± 25.4 % inhibition at 10 µM | C[C@H]1C2=CC(OC(C3=CC=CC=C3)=O)=C(C)C=C2/C=C(C)\CCC1 | 57 |

| | | | | |
|---|---|---|---|---|
| **AS88** | CHEMBL4542864 | 46.9 ± 5.3 % inhibition at 10 µM | OC1=C(C)C=C2C([C@H](C)CC[C@H]3[C@](C)(O3)C2)=C1 | [57] |
| **AS89** | CHEMBL4550701 | 47.9 ± 8.1 % inhibition at 10 µM | C[C@H]1C2=CC(OC(C3=CC=CC=C3)=O)=C(C)C=C2C[C@@](C)(O4)[C@@H]4CC1 | [57] |
| **AS90** | CHEMBL4553976 | 30.3 ± 5.4 % inhibition at 10 µM | OC1=C(C)C=C2C([C@H](C)CCC[C@@]3(C)[C@@H]2O3)=C1 | [57] |
| **AS91** | CHEMBL4538683 | 97.9 ± 15.3 % inhibition at 10 µM | C[C@H]1C2=CC(OC(C3=CC=CC=C3)=O)=C(C)C=C2[C@@H](O4)[C@]4(C)CCC1 | [57] |
| **AS92** | CHEMBL4567416 | 43.7 ± 27.5 % inhibition at 10 µM | OC1=C(C)C=C2C([C@](C)(O3)CC[C@H]3[C@H](C)C2)=C1 | [57] |
| **AS93** | CHEMBL4582836 | 26.1 ± 15.8 % inhibition at 10 µM | C[C@]1(O2)C3=CC(OC(C4=CC=CC=C4)=O)=C(C)C=C3C[C@@H](C)[C@@H]2CC1 | [57] |
| **AS94** | CHEMBL4578873 | 38.7 ± 2.5 % inhibition at 10 µM | OC1=C(C)C=C2C([C@@]3(C)CCC[C@H](C)[C@@H]2O3)=C1 | [57] |
| **AS95** | CHEMBL4593906 | 9.2 ± 4.1 % inhibition at 10 µM | C[C@]12C3=CC(OC(C4=CC=CC=C4)=O)=C(C)C=C3[C@@H](O2)[C@@H](C)CCC1 | [57] |

## 2. Description and optimisation of pharmacophore models

### Model SB1

Pharmacophore SB1 was derived from Nocodazole bound to chain B of porcine tubulin (PDB: 5CA1).[58] Based on the automatically generated pharmacophore model, removal and tolerance adjusting of features and Xvols coat modifications, led to the model consisting of two HC features and one HBD (interaction with GLU198B). LB pharmacophore features from active compounds **AS2**, **AS7**, **AS8**, **AS10** , and **AS11** were merged, and the feature coordinates were extracted and manually added to model SB1, leading to the final model consisting of an additional HBD, two HBAs, two AI features and eleven Xvols.

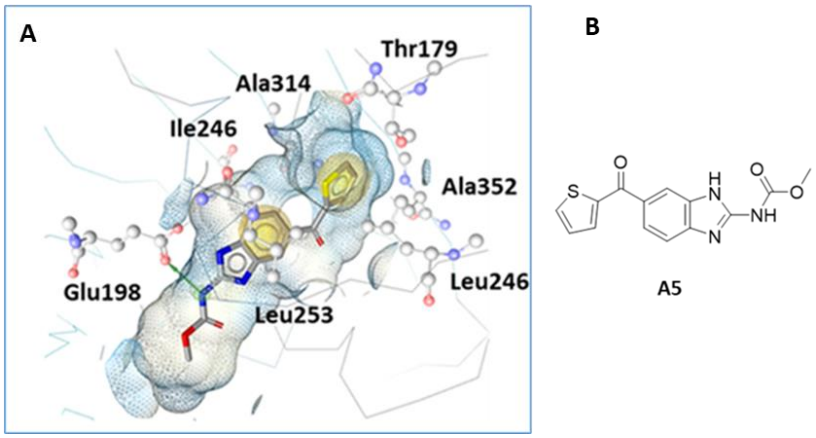


**Figure S1.** A) Automatically generated pharmacophore model of Tubulin CBS 3D crystal structure complex with nocodazole **AS5** based on (PDB 5CA1)[58], B) Structure of the ligand nocodazole **AS5**.

**Model SB2**

Pharmacophore model SB2 was derived from [2-(1H-indol-4-yl)-1H-imidazol-4-yl](3,4,5-trimethoxyphenyl)methanone bound to chain B of bovine tubulin (PDB: 6O5M).[59] Based on the automatically generated pharmacophore model, removal and tolerance adjusting of features and Xvols coat modifications, led to the model consisting of one HC feature, three HBAs towards HOH67B and Cys239B, two HBDs (interactions with Thr179A, ASN347B), and 18 Xvols.

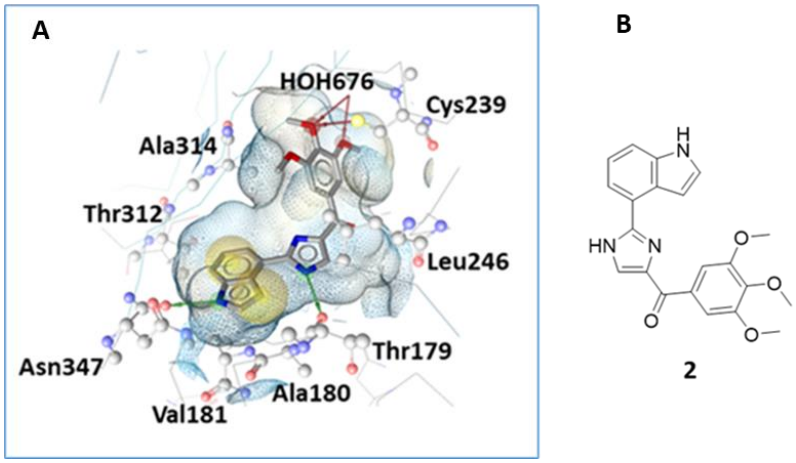


**Figure S2.** A) Automatically generated pharmacophore model of Tubulin CBS 3D crystal structure complex with the indol-imidazol-trimethoxypheny **2** based on (PDB 6O5M)[59], B) Structure of the ligand **2**.

**Model LB3**

Pharmacophore model LB3 was developed by automatic clustering of **AS55**, **AS56**, **AS57**, **AS63**, **AS85**, **AS86**, **AS87**, **AS88**, **AS89**, **AS90**, **AS91**, **AS92**, **AS93**, **AS94**, and **AS95** and creating a merged feature pharmacophore. After automatic pharmacophore model generation, removal and tolerance adjusting of features and Xvols coat modifications were optimised to find as many actives as possible while excluding inactives. The final model contained one AI feature, three HC features, two HBAs and 36 Xvols.

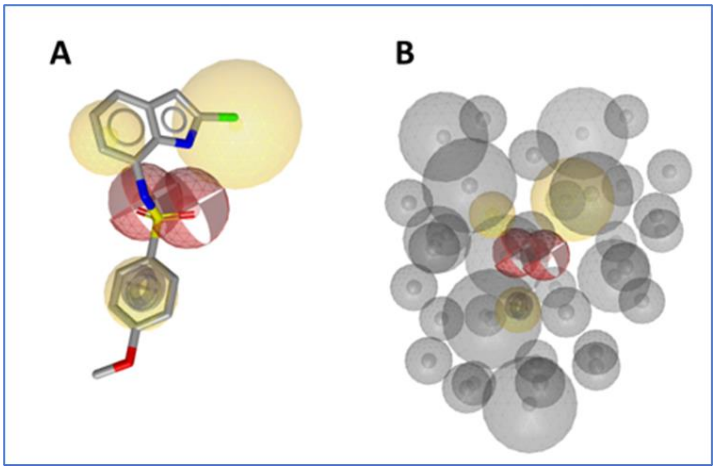


**Figure S3.** A) Optimised LB pharmacophore model LB3 aligned with base ligand **AS55** and B) the model LB3 with Xvols spheres. (HC, yellow spheres), (AI, purple sphere) Hydrogen bond (HBA; red arrows/spheres), and (Xvols; grey sphere).

**Model LB4**

Pharmacophore model LB4 was developed by automatic clustering and aligning the myosverin derivatives **AS66**, **AS67**, **AS68**, **AS69**, **AS70**, **AS71**, and **AS72** and creating a merged feature pharmacophore. After automatic pharmacophore model generation, removal and tolerance adjusting of features and Xvols coat modifications were optimised to find as many actives as possible while excluding inactives. The final model contained two HC features, five HBAs, two HBDs and 54 Xvols.

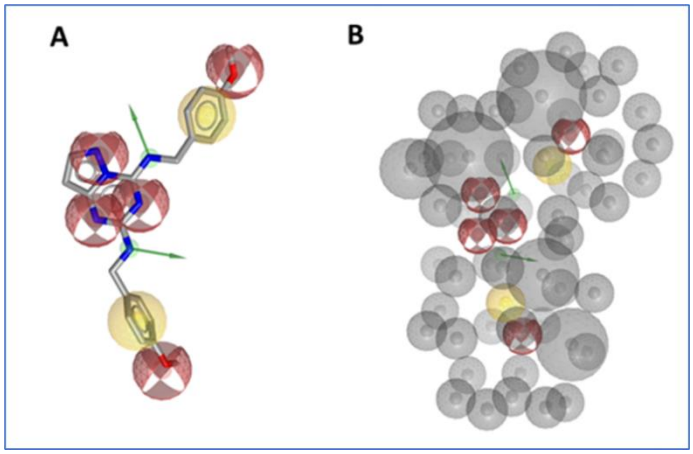


**Figure S4.** A) Optimised LB pharmacophore model LB4 aligned with base ligand **AS71** and B) the model LB4 with Xvol spheres. (HC, yellow spheres), (AI, purple sphere), (HBD; green arrows/spheres), Hydrogen bond acceptors (HBA; red arrows/spheres), and (Xvols; grey sphere).

**Model LB5**

Pharmacophore model LB5 was developed by automatic clustering and aligning the sesquiterpenoids **AS85, AS86**, **AS87**, **AS88**, **AS89**, **AS90**, **AS91**, **AS92**, **AS93**, and **AS94** and creating a merged features pharmacophore. After automatic pharmacophore model generation, removal and tolerance adjusting of features and Xvols coat modifications were optimised to find as many actives as possible while excluding inactives. The final model contained one AI feature, three HC features, one HBA, and 49 Xvols.

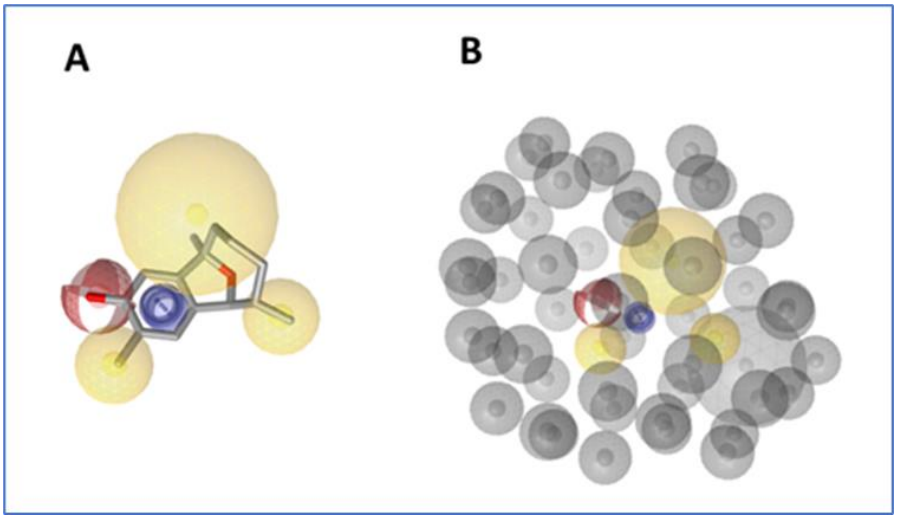


**Figure S5**. A) Optimised LB pharmacophore model LB5 aligned with base ligand **AS94** and B) the model LB5 with Xvols spheres. (HC, yellow spheres), (AI, purple sphere), (HBA; red arrows/spheres), and (Xvols; grey sphere).

**Model LB6**

Pharmacophore model LB6 was developed by manually selecting and aligning the indole-sulfonamide derivatives **AS58**, **AS59**, **AS60**, and **AS61**, creating a shared features pharmacophore. After automatic pharmacophore model generation, removal and tolerance adjusting of features and Xvols coat modifications were optimised to find as many actives as possible while excluding inactives. The final model contained two AI features, two HC features, two HBAs, one HBD and 35 Xvols.

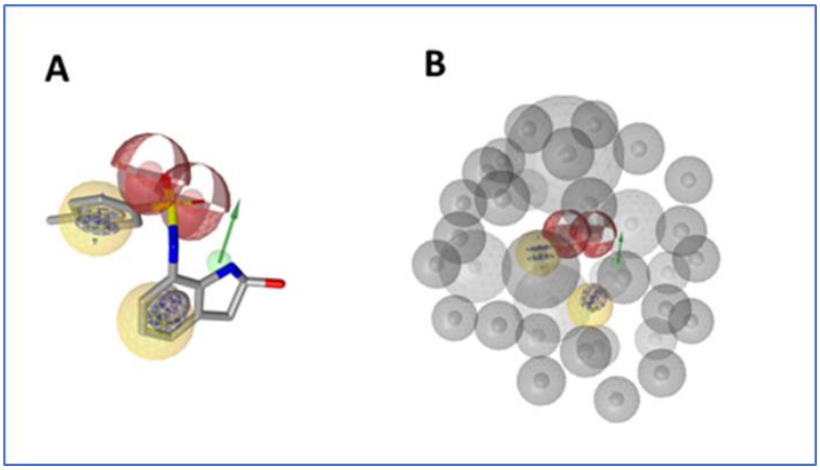


**Figure S6**. A) Optimised LB pharmacophore model LB6 aligned with base ligand **AS59** and B) the model LB6 with Xvol spheres. (HC, yellow spheres), (AI, purple sphere), (HBD; green arrows/spheres), (HBA; red arrows/spheres), and (Xvols; grey sphere).

**Model LB7**

Pharmacophore model LB7 was developed by manually selecting and aligning **AS30**, **AS33**, **AS34**, **AS75**, and **AS77** and creating a merged features pharmacophore. After automatic pharmacophore model generation, removal and tolerance adjusting of features and Xvols coat modifications were optimised to find as many actives as possible while excluding inactives. The final model contained one AI feature, one HC feature, four HBAs, one HBD and 68 Xvols.

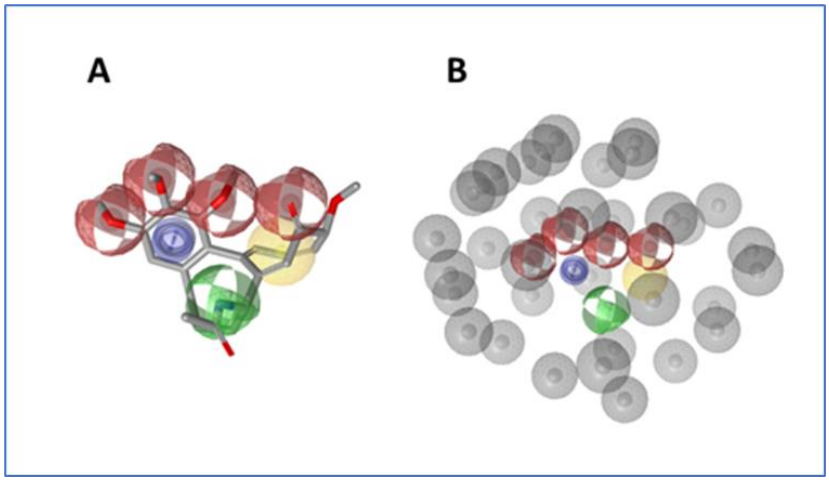


**Figure S7.** A) Optimised LB pharmacophore model LB7 aligned with base ligand **AS30** and B) the model LB7 with Xvols spheres. (HC, yellow spheres), (AI, purple sphere), (HBD; green arrows/spheres), (HBA; red arrows/spheres), and (Xvols; grey sphere).

**Model LB8**

Pharmacophore model LB8 was developed bymanually selectingand aligning **AS1**, **AS3**, **AS8**, **AS12**, **AS13**, **AS14**, **AS15**, **AS16**, and **AS17** and creating a merged features pharmacophore. After automatic pharmacophore model generation, removal and tolerance adjusting of features and Xvols coat modifications were optimised to find as many actives as possible while excluding inactives. The final model contained one AI feature, two HC features, two HBAs and 30 Xvols.

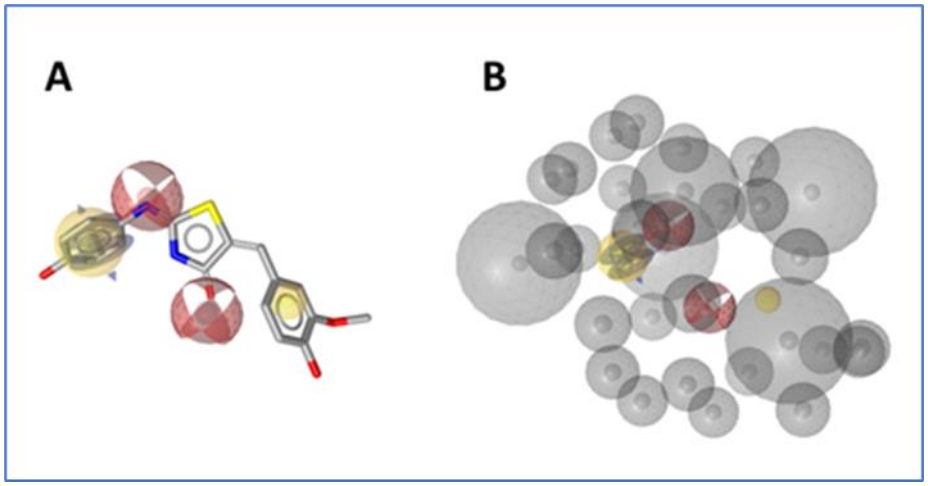


**Figure S8.** A) Optimised LB pharmacophore model LB8 aligned with base ligand **AS15** and B) the model LB8 with Xvol spheres. (HC, yellow spheres), (AI, purple sphere), (HBA; red arrows/spheres), and (Xvols; grey sphere).

**Model LB9**

Pharmacophore model LB9 was developed by manually selecting and aligning **AS3**, **AS8**, **AS12**, and **AS13** and creating a merged features pharmacophore. After automatic pharmacophore model generation, removal and tolerance adjusting of features and Xvols coat modifications were optimised to find as many actives as possible while excluding inactives. The final model contained two AI features, one HC feature, three HBAs and 39 Xvols.

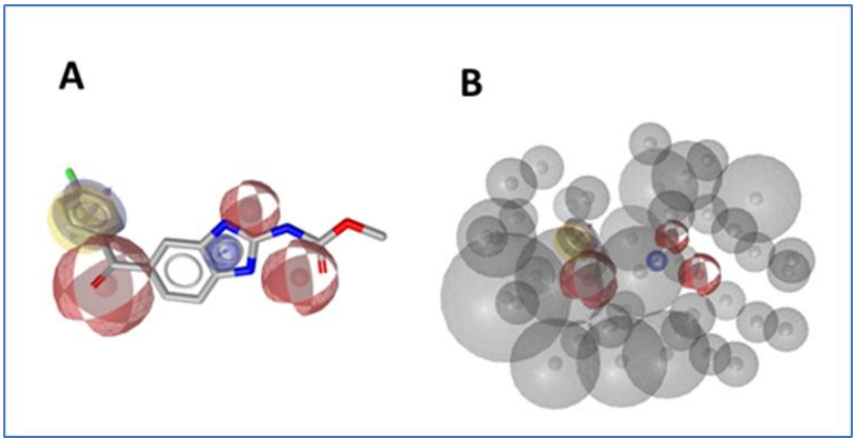


**Figure S9**. A) Optimised LB pharmacophore model LB9 aligned with base ligand **AS8** and B) the model LB9 with Xvols spheres. (HC, yellow spheres), (AI, purple sphere), (HBA; red arrows/spheres), and (Xvols; grey sphere).

**Model LB10**

Pharmacophore model LB10 was developed by automatic clustering and aligning **AS79**, **AS80**, **AS81**, and **AS82** creating a merged features pharmacophore. After automatic pharmacophore model generation, removal and tolerance adjusting of features and Xvols coat modifications were optimised to find as many actives as possible while excluding inactives. The final model contained two AI features, two HC features, two HBAs and 45 Xvols.

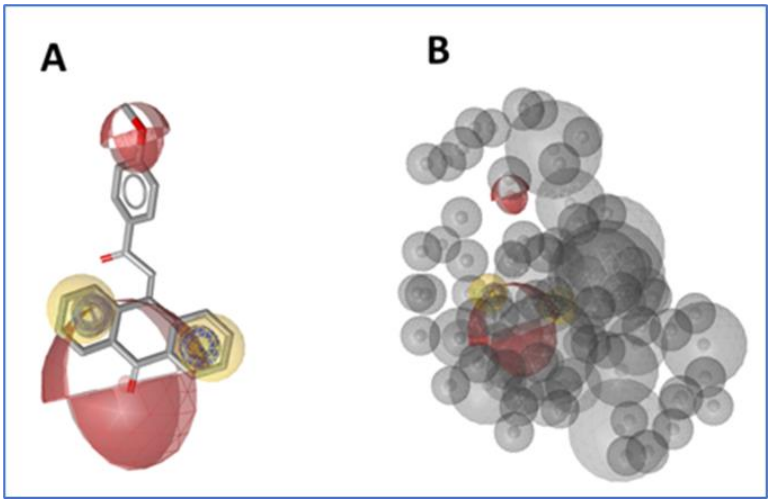


**Figure S10**. A) Optimised LB pharmacophore model LB10 aligned with base ligand **AS80** and B) the model LB10 with Xvol spheres. (HC, yellow spheres), (AI, purple sphere), (HBA; red arrows/spheres), and (Xvols; grey sphere).

**Model LB11**

Pharmacophore model LB11 was developed by manually selecting and aligning **AS13**, **AS27**, **AS43**, and **AS72** and creating a merged features pharmacophore. After automatic pharmacophore model generation, removal and tolerance adjusting of features and Xvols coat modifications were optimised to find as many actives as possible while excluding inactives. The final model contained one HC feature, four HBAs and 39 Xvols.

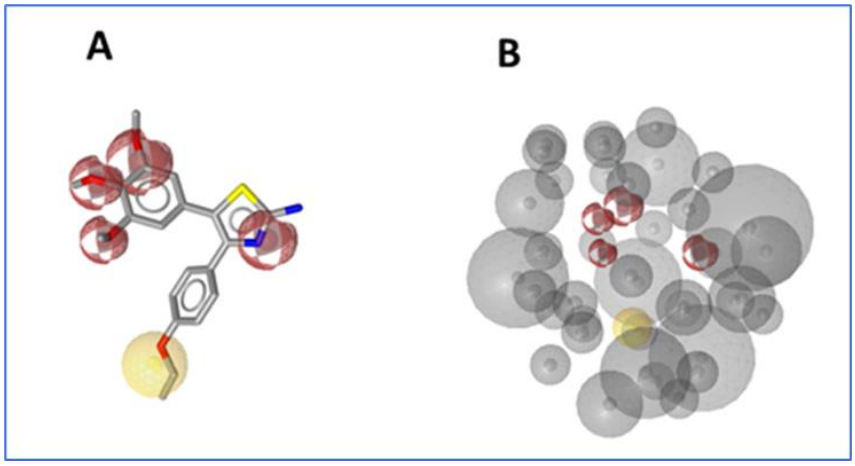


**Figure S11.** A) Optimised LB pharmacophore model LB11 aligned with base ligand **AS13** and B) the model LB11 with Xvol spheres. (HC, yellow spheres), (AI, purple sphere), (HBA; red arrows/spheres), and (Xvols; grey sphere).

**Model DS2**

The model DS2 was based on **AS64**, a diphenyl sulfonamide. It contained three HC features, two AI features that are mapped on the two phenyl rings, two HBD features and 26 Xvols.

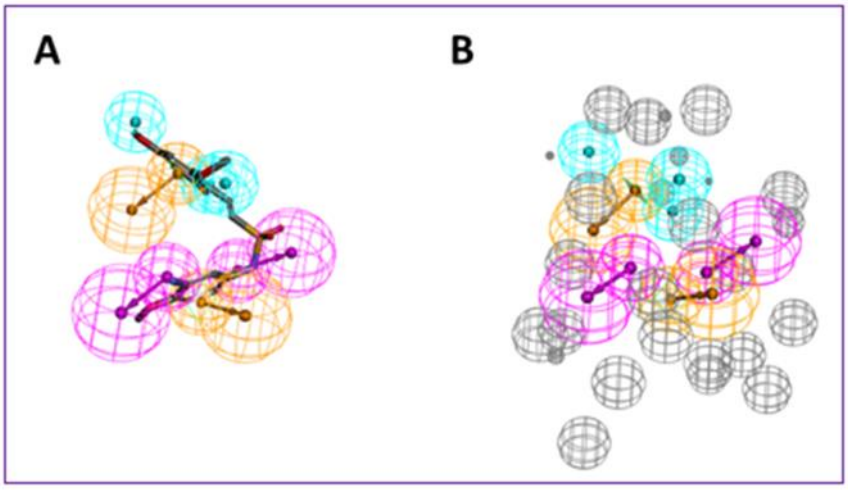


**Figure S12.** A) Optimised LB pharmacophore model DS2 aligned with base ligand **AS64**. B) the model DS2 with Xvol spheres. (HC, blue spheres), (AI, brown spheres), (HBD; purple), and (Xvols; grey sphere).

**Model DS5**

Model DS5 was based on **AS75**, a podophyllotoxin. It contains four HC features, two AI features, five HBA features and 34 Xvols.

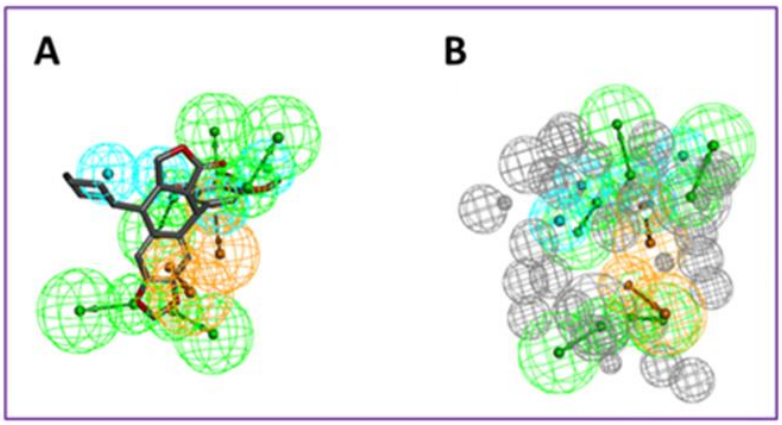


**Figure S13.** A) Optimised LB pharmacophore model DS5 aligned with base ligand **AS75**. B) the model DS5 with Xvol spheres. (HC, blue spheres), (AI, brown spheres), (HBA; green sphere), and exclusion volumes (Xvols; grey sphere).

**Model DS8**

The model DS8 was calculated for **AS77**, a modified podophyllotoxin scaffold with an amine functionality inserted in the central ring and an elongated linker to the trimethoxyphenylring.

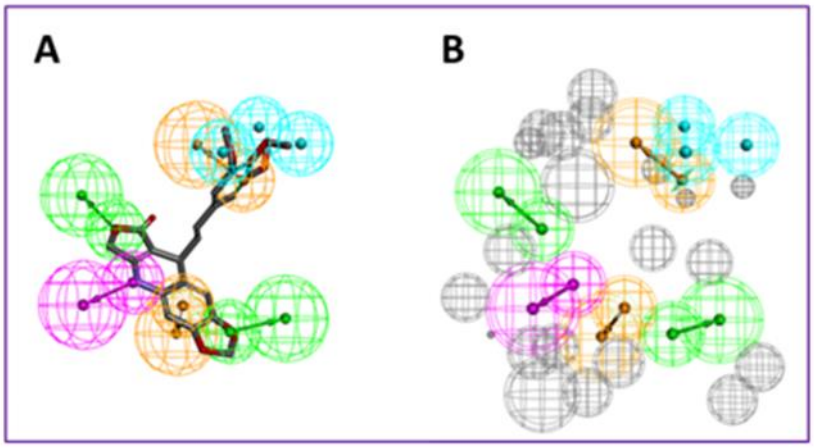


**Figure S14.** A) Optimised LB pharmacophore model DS8 aligned with base ligand **AS77** .B) the model DS8 with Xvol spheres. (HC, blue spheres), (AI, brown spheres), (HBA; green sphere) (HBD; purple sphere), and (Xvols; grey sphere).

**Model DS9**

Model DS9 was derived from **AS79**, an anthracene sulfonate. It consists of a HC feature, three AI features, two HBA features and 60 Xvols.

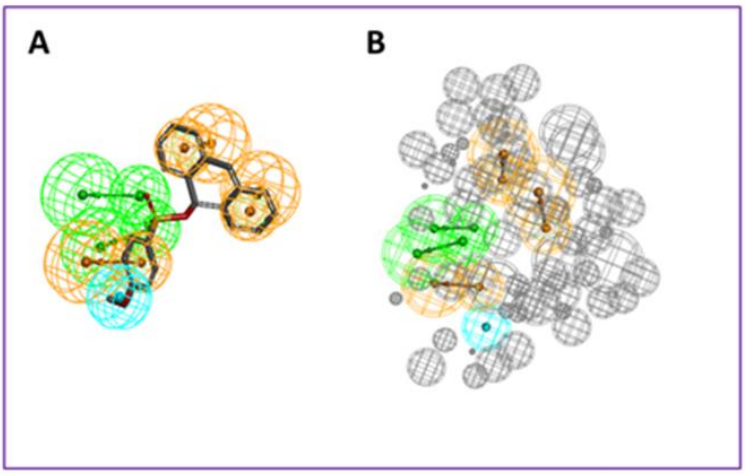


**Figure S15**. A) Optimised LB pharmacophore model DS9 aligned with base ligand **AS79**. B) the model DS9 with Xvol spheres. (HC, blue spheres), (AI, brown spheres), (HBA; green sphere), and (Xvols; grey sphere).

**Model DS12**

The model DS12 was based on **AS29**, a chalcone. The final model contains two HC, two AI, two HBA features and 118 Xvols.

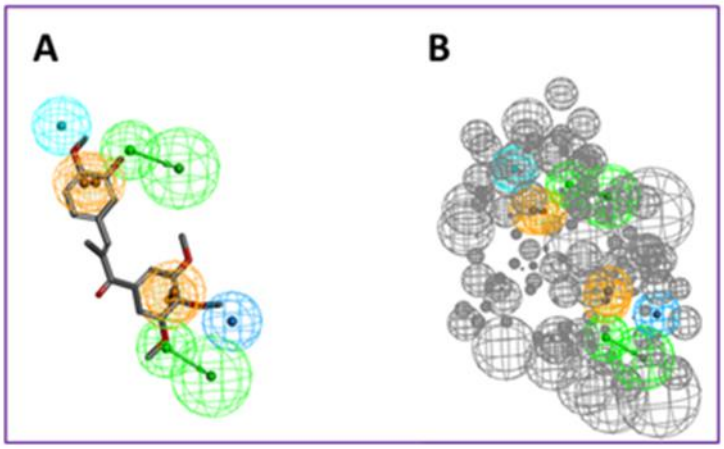


**Figure S16.** A) Optimised LB pharmacophore model DS12 aligned with base ligand **AS29**. B) the model DS12 with Xvol spheres. (HC, blue spheres), (AI, brown spheres), (HBA; green sphere), and (Xvols; grey sphere).

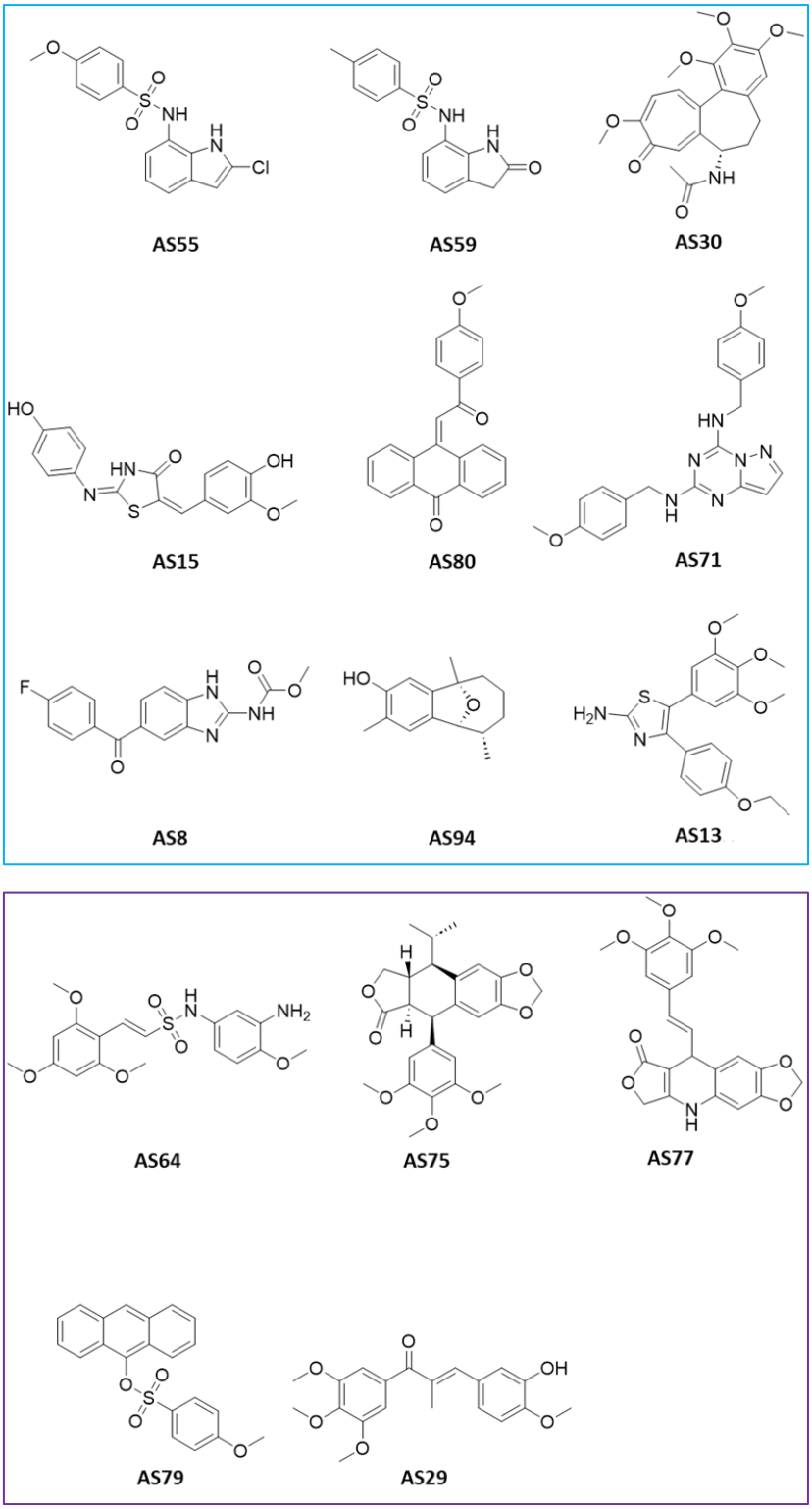


**Figure S17.** Chemical structures of the main active scaffolds used to generate the LB pharmacophore models. Compounds in the blue box were used for the LS models and compounds in the purple box were used for the DS models.

3. Virtual screening of pharmacophore models with consensus hits

**Table S2.** Virtual screening results with consensus hits obtained by the respective pharmacophore models.

| | **Consensus hit** | **(n=2)** | |
|---|---|---|---|
| Models | Specs (Synth) | Specs (NP) | PhytoChem (PC) |
| DS2/DS8 | 0 | 0 | 1 |
| DS5/DS8 | 0 | 3 | 0 |
| DS8/DS9 | 4 | 1 | 0 |
| DS5/DS9 | 9 | 0 | 0 |
| DS2/DS9 | 13 | 0 | 0 |
| DS12/DS9 | 5 | 0 | 0 |
| DS12/DS2 | 3 | 0 | 0 |
| LB8/DS9 | 3 | 0 | 0 |
| LB8/DS2 | 1 | 0 | 0 |
| LB8/DS12 | 2 | 0 | 0 |
| LB7/DS9 | 2 | 0 | 0 |
| LB6/DS9 | 1 | 0 | 0 |
| LB5/DS9 | 19 | 0 | 0 |
| LB5/DS2 | 10 | 0 | 0 |
| LB5/DS12 | 3 | 0 | 0 |
| LB5/DS8 | 4 | 0 | 0 |
| LB5/DS6 | 3 | 0 | 0 |
| LB3/DS9 | 46 | 0 | 0 |
| LB3/DS5 | 1 | 0 | 0 |
| LB3/DS2 | 5 | 0 | 0 |
| LB3/DS12 | 3 | 0 | 0 |
| LB3/LB9 | 1 | 0 | 0 |
| LB3/LB8 | 4 | 0 | 0 |
| LB3/LB6 | 16 | 0 | 0 |
| LB3/LB5 | 167 | 0 | 0 |
| SB2/LB5 | 4 | 0 | 0 |
| LB11/DS9 | 6 | 0 | 0 |
| LB11/DS2 | 1 | 0 | 0 |
| LB11/DS12 | 1 | 0 | 0 |
| LB11/LB9 | 1 | 0 | 0 |
| LB11/LB8 | 1 | 0 | 0 |
| LB11/LB7 | 1 | 0 | 0 |

| | | | |
|---|---|---|---|
| LB11/LB6 | 6 | 0 | 0 |
| LB11/LB5 | 5 | 0 | 0 |
| LB11/LB3 | 6 | 0 | 0 |
| LB11/SB2 | 3 | 0 | 0 |
| LB10/DS9 | 6 | 0 | 0 |
| LB10/DS5 | 5 | 0 | 0 |
| LB10/LB3 | 2 | 0 | 0 |
| LB10/LB11 | 3 | 0 | 0 |
| SB1/LB5 | 4 | 0 | 0 |
| SB1/LB3 | 1 | 0 | 0 |
| | **Consensus hit** | **(n=3)** | |
| Models | Specs (Synth) | Specs (NP) | PhytoChem (PC) |
| DS5/DS8/DS9 | 0 | 3 | 0 |
| LB10 / LB5 /DS9 | 1 | 0 | 0 |
| LB10 / DS9/DS12 | 2 | 0 | 0 |
| LB11 /LB6/DS2 | 1 | 0 | 0 |
| LB3/LB5/LB8 | 1 | 0 | 0 |
| LB3/LB5/DS9 | 2 | 0 | 0 |
| LB5/DS2/DS8 | 1 | 0 | 0 |
| DS2/DS5/DS9 | 1 | 0 | 0 |
| LB3/LB5/DS2 | 1 | 0 | 0 |

4. Test compound selection of hits obtained from virtual screening of the databases.

**Table S3.** Virtual screening hits selected for experimental validation. Red box indicates insoluble compounds or fluorescent interference and thus excluded compounds.

| Specs | Virtual Hit | SB1 | SB2 | LB3 | LB4 | LB5 | LB6 | LB7 | LB8 | LB9 | LB10 | LB11 | DS2 | DS5 | DS8 | DS9 | DS12 |
|---|---|---|---|---|---|---|---|---|---|---|---|---|---|---|---|---|---|
| AA-504/21163091 | SC1 | | | | | | | | | | | | | ☒ | | | |
| AB-323/13887441 | SC2 | | ☒ | | | | | | | | | | | | | | |
| AC-776/41252593 | SC3 | | | | | | | | | | | | | ☒ | | | |
| AF-399/14738025 | SC4 | | | | | | | | ☒ | | | | | | | | |
| AG-205/13184005 | SC5 | | | ☒ | | | | | | | | | | | | | |
| AG-205/21054014 | SC6 | | | | | | | | | | | | | | | ☒ | |
| AG-205/36265044 | SC7 | ■ | | | | | | | | ☒ | | | | | | | |
| AG-389/15452424 | SC8 | | | | | | | | | | | | | | | | |
| AG-401/30827061 | SC9 | | | | | | | ■ | ■ | | | | | | | | ■ |
| AG-690/09788017 | SC10 | | | | | | | | | | ■ | | | | | | |
| AJ-292/21122017 | SC11 | | | | | | | | | | | | | ☒ | | | |
| AJ-916/12583009 | SC12 | | | | | ■ | | | ■ | | | | | | | | |
| AK-087/42718249 | SC13 | | | | | ☒ | | | | | | | | | | | |
| AK-087/42718376 | SC14 | | | | | | | | | | | | | | | ☒ | |
| AK-693/40962733 | SC15 | | | | | ☒ | | | | | | | | | | | |

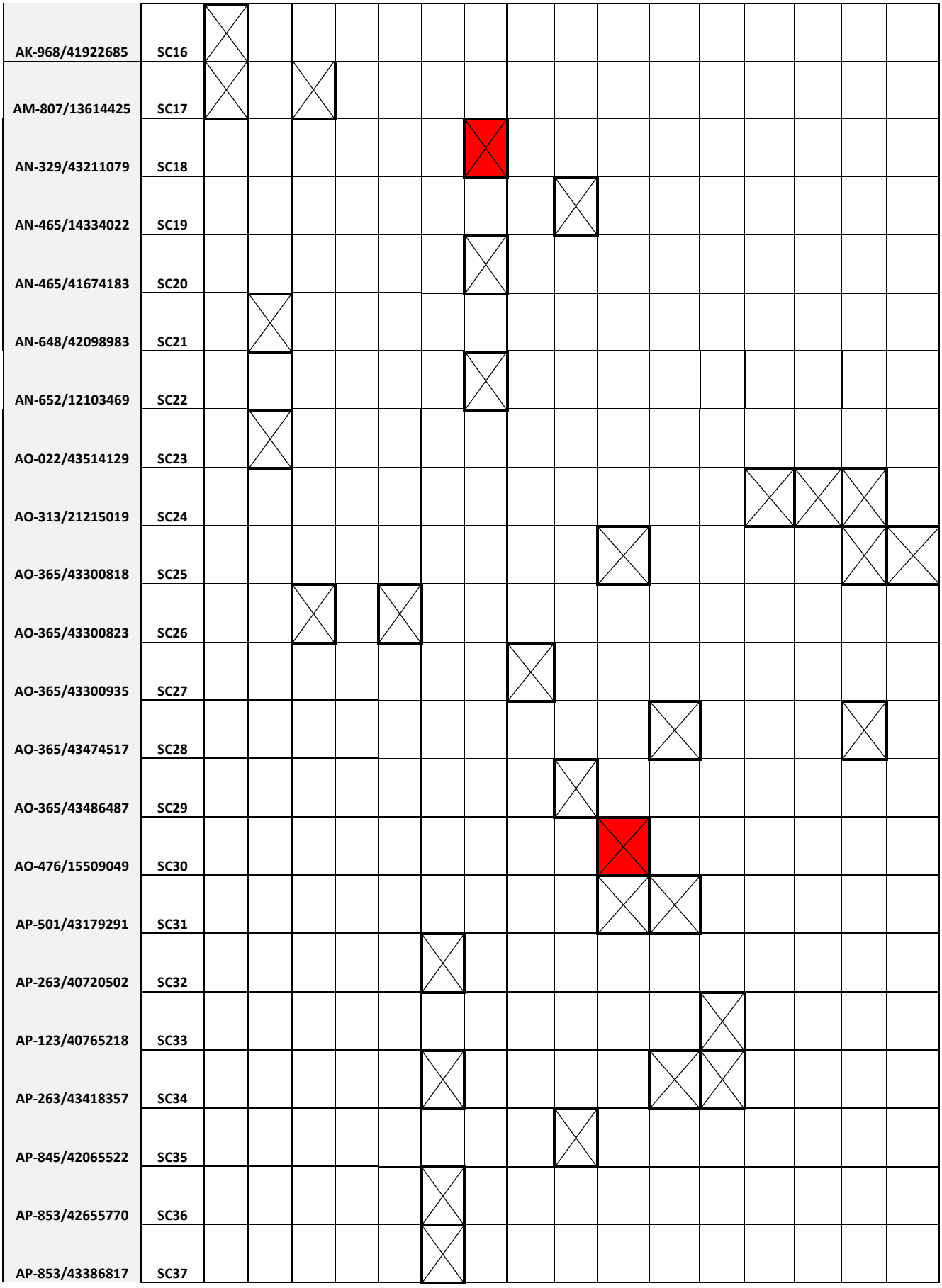
AK-968/41922685 SC16
AM-807/13614425 SC17
AN-329/43211079 SC18
AN-465/14334022 SC19
AN-465/41674183 SC20
AN-648/42098983 SC21
AN-652/12103469 SC22
AO-022/43514129 SC23
AO-313/21215019 SC24
AO-365/43300818 SC25
AO-365/43300823 SC26
AO-365/43300935 SC27
AO-365/43474517 SC28
AO-365/43486487 SC29
AO-476/15509049 SC30
AP-501/43179291 SC31
AP-263/40720502 SC32
AP-123/40765218 SC33
AP-263/43418357 SC34
AP-845/42065522 SC35
AP-853/42655770 SC36
AP-853/43386817 SC37

| | | | | | | | | | | | | | | | | | |
|---|---|---|---|---|---|---|---|---|---|---|---|---|---|---|---|---|---|
| AQ-086/43467809 | SC38 | X | | | | | | | | | | | | | | | |
| AT-057/43469212 | SC39 | | | | | | | | | | | | | | | | |
| AT-057/43485534 | SC40 | | | | | | | X | | | | | | | | | |
| AT-583/41299652 | SC41 | | | | | | | | | | | | | | X | | |
| AH-487/41949628 | SC42 | | | | | | | | | | | | | | | | X |
| AG-690/12094002 | SC43 | | | X | | | | | X | | | | | | | | |
| AI-204/31688027 | SC44 | | | | | | X | | | | | | | | | | |
| AG-690/12413358 | SC45 | X | | X | | | | | | | | | | | | | |
| AI-899/21033027 | SC46 | | | | | | | | | | X | | | | | | |

## 5. Bioactivity results of selected test compounds from the polymerisation inhibition assay and similarity prediction

**Table S4**. Overview of the tubulin polymerisation inhibition screening results.

| Specs ID-number | ID | % Inhibition (30 µM) ± SD | % Inhibition (10 µM) ± SD *20 µM | IC50 (µM) |
|---|---|---|---|---|
| AA-504/21163091 | SC1 | 28.8 ± 22.7 | n.d | n.d |
| AB-323/13887441 | SC2 | ≤ 0 | n.d | n.d |
| AC-776/41252593 | SC3 | Insoluble | ≤ 0 | n.d |
| AF-399/14738025 | SC4 | 7.0 ± 8.1 | n.d | n.d |
| AG-205/13184005 | SC5 | ≤ 0 | n.d | n.d |
| AG-205/21054014 | SC6 | 38.4 ± 12.6 | n.d | n.d |
| AG-205/36265044 | SC7 | insoluble | insoluble | n.d |
| AG-389/15452424 | SC8 | Insoluble | ≤ 0 | n.d |
| AG-401/30827061 | SC9 | Insoluble | Insoluble | n.d |
| AG-690/09788017 | SC10 | Insoluble | Insoluble | n.d |
| AJ-292/21122017 | SC11 | ≤ 0 | n.d | n.d |
| AJ-916/12583009 | SC12 | insoluble | insoluble | n.d |
| AK-087/42718249 | SC13 | ≤ 0 | n.d | n.d |
| AK-087/42718376 | SC14 | insoluble | 43.9 ± 23.9 | n.d |
| AK-693/40962733 | SC15 | n.d | ≤ 0 | n.d |
| AK-968/41922685 | SC16 | n.d | ≤ 0 | n.d |
| AM-807/13614425 | SC17 | n.d | 1.7 ± 3.1 | n.d |
| AN-329/43211079 | SC18 | n.d | n.d | n.d |
| AN-465/14334022 | SC19 | n.d | ≤ 0 | n.d |
| AN-465/41674183 | SC20 | 19. 2 ± 24.9 | n.d | n.d |
| AN-648/42098983 | SC21 | n.d | 1.29 ± 1.28 | n.d |
| AN-652/12103469 | SC22 | 54.7 ± 2.5 | n.d | n.d |
| AO-022/43514129 | SC23 | 99.3 ± 3.72 | 86.5 ± 2.7 | Yes |
| AO-313/21215019 | SC24 | insoluble | *95.50 ± 2.5 | n.d |
| AO-365/43300818 | SC25 | 25.5 ± 14.6 | n.d | n.d |
| AO-365/43300823 | SC26 | insoluble | 37.6 ± 35.9 | n.d |
| AO-365/43300935 | SC27 | 32.87 ± 1.69 | 36.0 ± 4.4 | n.d |
| AO-365/43474517 | SC28 | Insoluble | 2.33 ± 1.8 | n.d |
| AO-365/43486487 | SC29 | 8.69 ± 4.42 | n.d | n.d |
| AO-476/15509049 | SC30 | Insoluble | Insoluble | n.d |
| AP-501/43179291 | SC31 | Insoluble | ≤ 0 | n.d |
| AP-263/40720502 | SC32 | 73.9 ± 0.2 | n.d | n.d |
| AP-123/40765218 | SC33 | ≤ 0 | n.d | n.d |

| | | | | |
|---|---|---|---|---|
| AP-263/43418357 | SC34 | 37.8 ± 5.7 | n.d | n.d |
| AP-845/42065522 | SC35 | Insoluble | 7.6 ± 8.0 | n.d |
| AP-853/42655770 | SC36 | Insoluble | ≤ 0 | n.d |
| AP-853/43386817 | SC37 | 100.3 ± 0.4 | 71.3 ± 6.4 | Yes |
| AQ-086/43467809 | SC38 | Insoluble | 6.7 ± 1.0 | n.d |
| AT-057/43469212 | SC39 | Insoluble | ≤ 0 | n.d |
| AT-057/43485534 | SC40 | Insoluble | 3.9 ± 7.3 | n.d |
| AT-583/41299652 | SC41 | ≤ 0 | n.d | n.d |
| AH-487/41949628 | SC42 | ≤ 0 | n.d | n.d |
| AG-690/12094002 | SC43 | Insoluble | 11.3 ± 3.5 | n.d |
| AI-204/31688027 | SC44 | 8.84 ± 1.45 | n.d | n.d |
| AG-690/12413358 | SC45 | Insoluble | 17.7 ± 1.0 | n.d |
| AI-899/21033027 | SC46 | 8.3 ± 2.4 | n.d | n.d |
| MERCK Group | Hit47 | ≤ 0 | n.d | n.d |
| TCI Chemicals | Colchicine | 98.8 ± 5.2 | 83.2 ± 1.7 | YES |

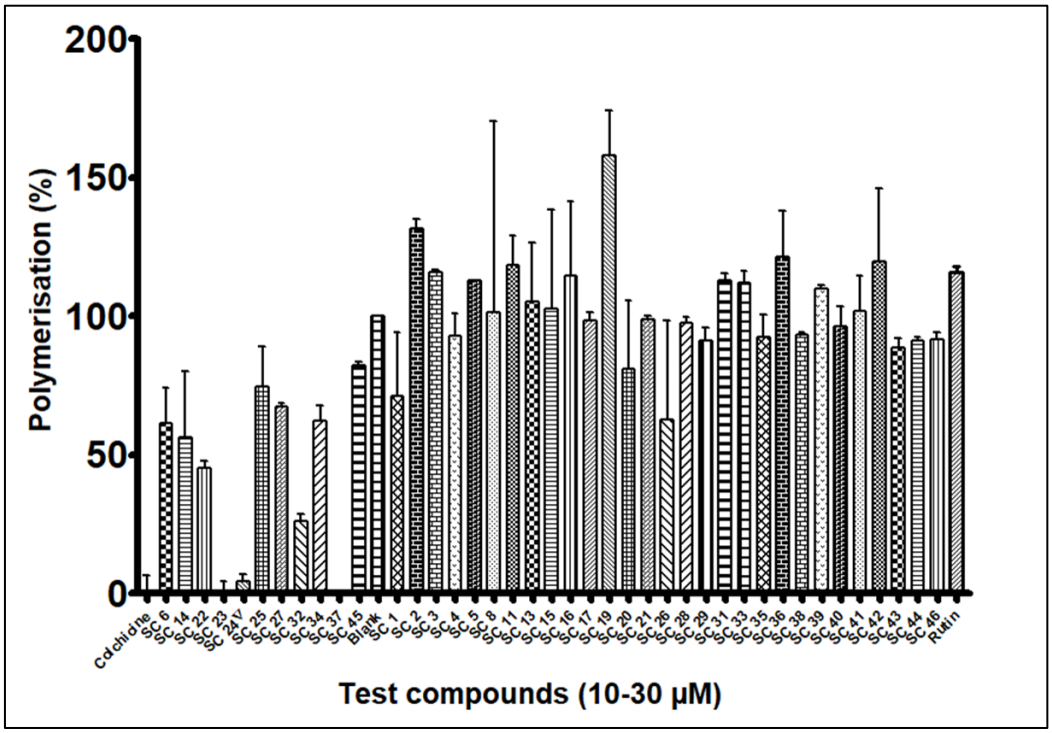


**Figure S18**. Graphical results of the active/inactive preliminary screening. Corresponding numerical values are shown above in Table S4.

**Table S5.** SwissTarget Similarity prediction scores for the tubulin inhibitors

| Inhibitor | Tubulin-Ligand Probability Score | Best Target Probability score | CHEMBL Target ID |
|---|---|---|---|
| SC6 | none | Carbonic anhydrase II (0.04) | CHEMBL205 |
| SC14 | CHEMBL195840 (0.62) | - | CHEMBL1915 |
| SC22 | none | Phosphodiesterase 5A (0.11) | CHEMBL1827 |
| SC23 | none | Acetyl-CoA carboxylase 2 (0.11) | CHEMBL4829 |
| SC24 | CHEMBL363063 (0.90) | - | CHEMBL1915 |
| SC25 | none | NAD-dependent deacetylase sirtuin 1 (0.14) | CHEMBL4506 |
| SC27 | none | NAD-dependent deacetylase sirtuin 1 (0.21) | CHEMBL4506 |
| SC32 | none | Metabotropic glutamate receptor 5 (0.11) | CHEMBL3227 |
| SC34 | none | Microtubule-associated protein tau (0.79) | CHEMBL1293224 |
| SC37 | none | Monoamine oxidase B (0.11) | CHEMBL2039 |
| SC45 | none | Histone deacetylase 1 0.12) | CHEMBL325 |

## 6. Active compound characterization provided by Specs

**Table S6**. List of compound characterization data for the found active inhibitors provided by SPECS.

| ID | Specs ID | QC Method | Purity | MW | SMILES |
|---|---|---|---|---|---|
| SC6* | AG-205/21054014 | LC-MS | >95% | 730.7 | CC1=CC(=O)Oc2cc(ccc12)OC6OC(COS(O)(=O)=O)C(OC(=O)c3ccccc3)C(OC(=O)c4ccccc4)C6(OC(=O)c5ccccc5) |
| SC14 | AK-087/42718376 | H-NMR,LC-MS | >95% | 346.38 | Oc3ccc(C(=O)C=Cc2ccccc2(OCc1ccccc1))c(O)c3 |

| | | | | | |
|---|---|---|---|---|---|
| SC22 | AN-652/12103469 | H-NMR,LC-MS | 95% | 401.46 | CCOC(=O)c2ccccc2(NC(=O)c1cc(OCC)c(OCC)c(c1)OCC) |
| SC23 | AO-022/43514129 | LC-MS | >95% | 445.4 | O=C(CC1NC(=O)c2ccccc2(NC1(=O)))NCCn3c4ccccc4(nc3C(F)(F)F) |
| SC24 | AO-313/21215019 | H-NMR,LC-MS | 95% | 551.98 | COc1cc(cc(OC)c1(OC))C5c2cc6OCOc6(cc2C(NC(=O)c3ccccc3Cl)C4COC(=O)C45) |
| SC25 | AO-365/43300818 | LC-MS | >95% | 328.35 | COc1ccc(cc1)OCC3=Nn2c(nnc2S3)c4ccco4 |
| SC27 | AO-365/43300935 | H-NMR,LC-MS | 95% | 298.33 | COc1ccccc1C3=Nn2c(nnc2S3)c4ccco4 |
| SC32 | AP-263/40720502 | LC-MS | >95% | 449.12 | CC(=O)Nc2ccccc2(OS(=O)(=O)c1cc(ccc1Br)Br) |
| SC34 | AP-263/43418357 | LC-MS | >95% | 348.2 | COc1c(ccc(c1Cl)Cl)S(=O)(=O)Nc2cccc(O)c2 |
| SC37 | AP-853/43386817 | H-NMR,LC-MS | 95% | 389.82 | O=C(CSc1nnc(o1)c2cccc(c2)Cl)Nc3ccc4OCOc4(c3) |
| SC45 | AG-690/12413358 | H-NMR,LC-MS | >95% | 525.4 | COc1ccc(cc1)NC(=O)c2ccc(cc2)Nc4nc3ccc(cc3c(n4)c5ccccc5)Br |

** Stereochemistry undefined*

## 7. LC-MS and $^{1}$H-NMR data provided by Specs

Compound **SC6**, LC-MS:

**Sample Report (continued):**

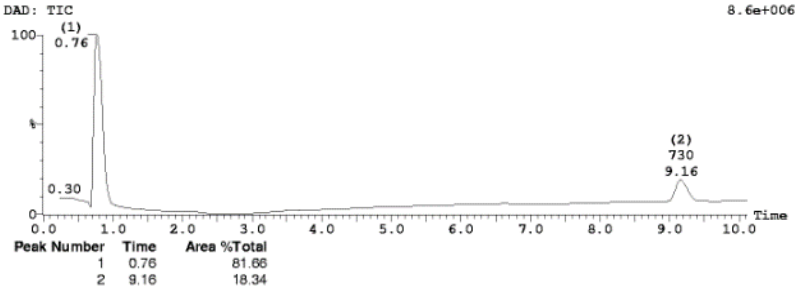


| Peak Number | Time | Area | %Total |
|---|---|---|---|
| 1 | 0.76 | | 81.66 |
| 2 | 9.16 | | 18.34 |

| Peak ID | Time | Mass Found | BPM |
|---|---|---|---|
| 1 | 0.76 | | 302.0 |

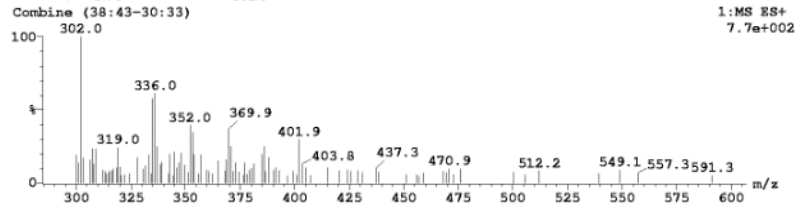


| Peak ID | Time | Mass Found | BPM |
|---|---|---|---|
| 2 | 9.16 | 730.14 | 748.3 |

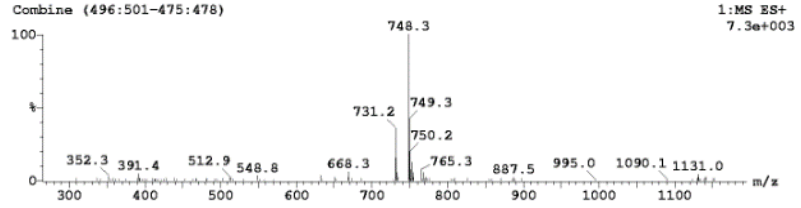


Compound **SC6**, $^{1}$H-NMR:

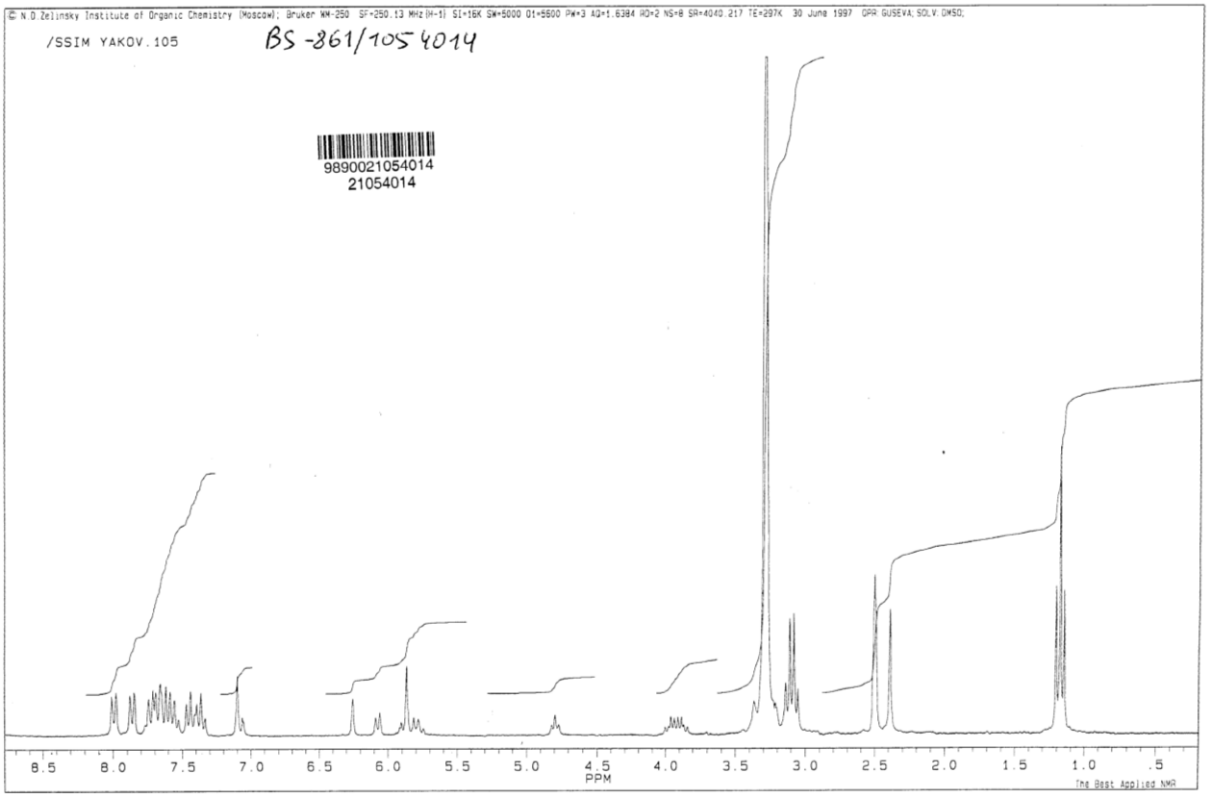


Compound **SC14**, LC-MS:

**Sample Report (continued):**

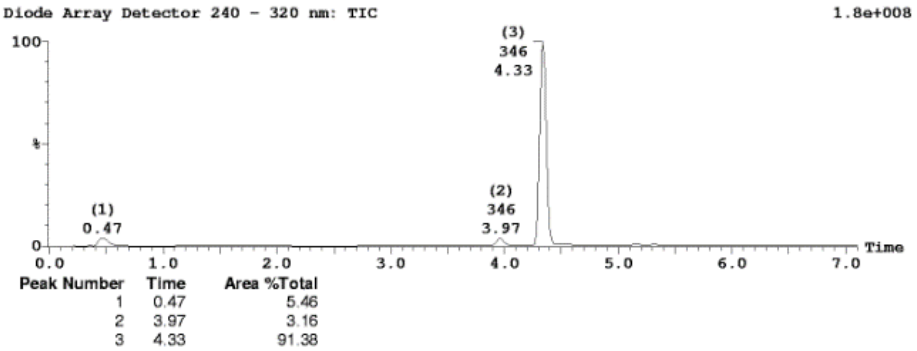


| Peak Number | Time | Area %Total |
|---|---|---|
| 1 | 0.47 | 5.46 |
| 2 | 3.97 | 3.16 |
| 3 | 4.33 | 91.38 |

| Peak ID | Time | Mass Found | BPM |
|---|---|---|---|
| 2 | 3.97 | 346.12 | 347 |

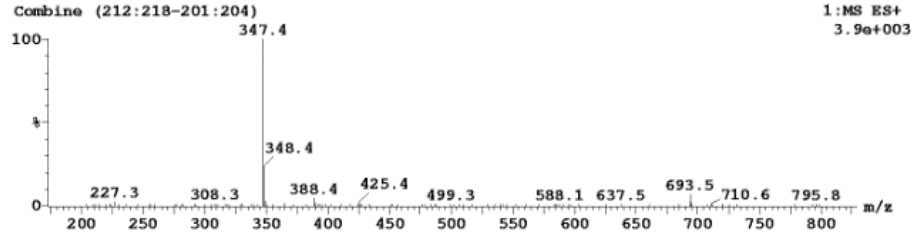


| Peak ID | Time | Mass Found | BPM |
|---|---|---|---|
| 3 | 4.33 | 346.12 | 347 |

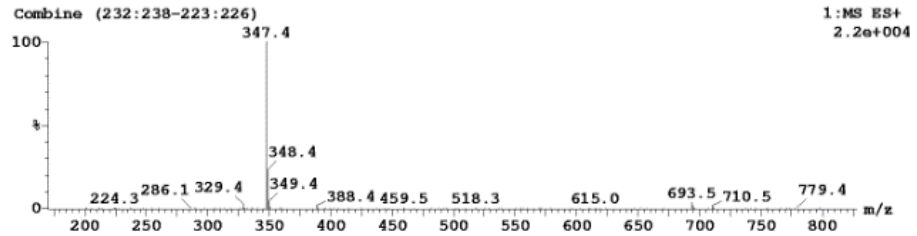


Compound **SC14**, $^{1}$H-NMR:

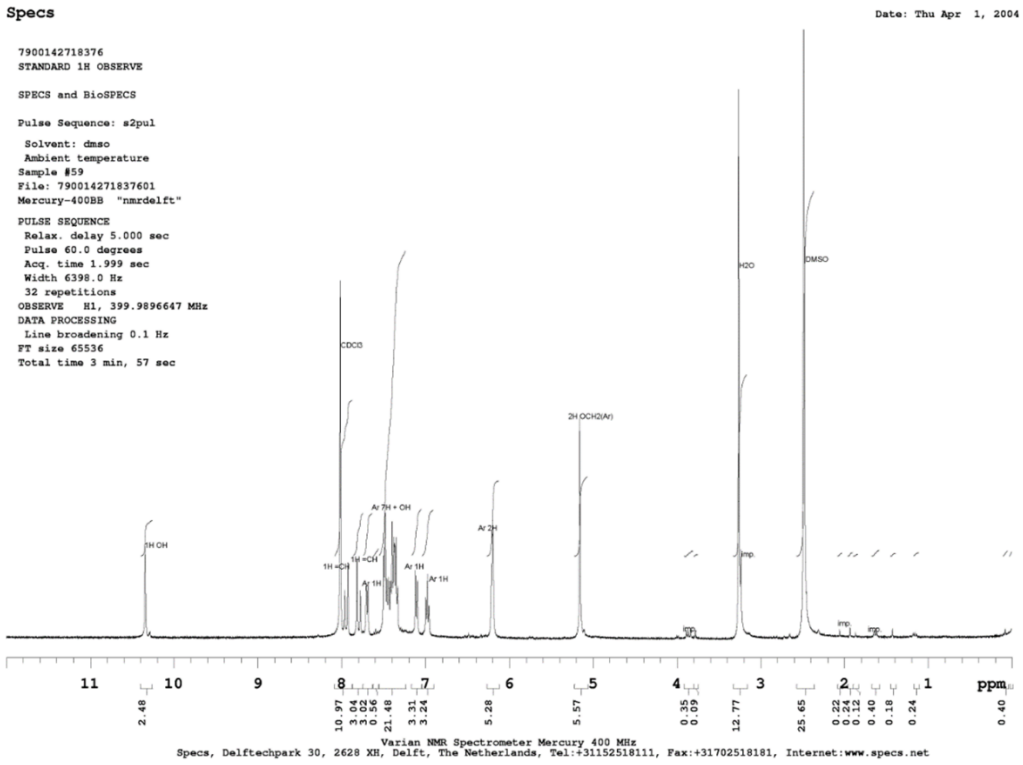


Compound **SC22**, LC-MS:

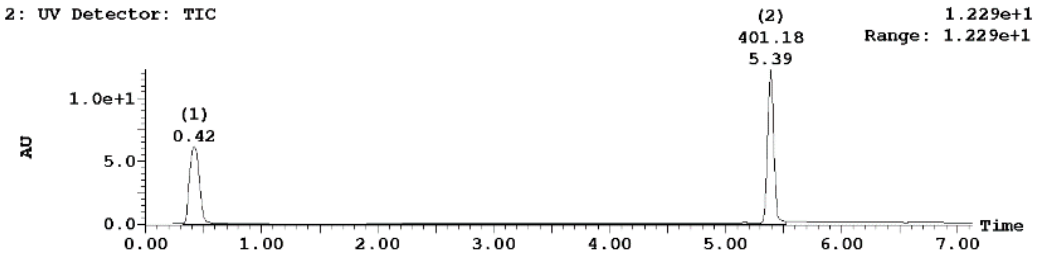


| Peak Number | Time | Area %Total |
|---|---|---|
| 1 | 0.42 | 44.18 |
| 2 | 5.39 | 55.82 |

| Peak ID | Time | Mass Found | BPM |
|---|---|---|---|
| 1 | 0.42 | | 223.25 |

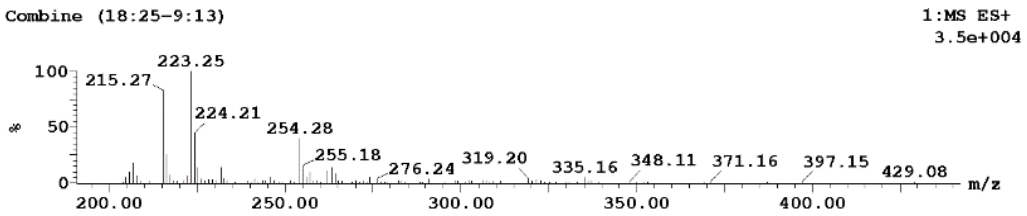


| Peak ID | Time | Mass Found | BPM |
|---|---|---|---|
| 2 | 5.39 | 401.18 | 402.36 |

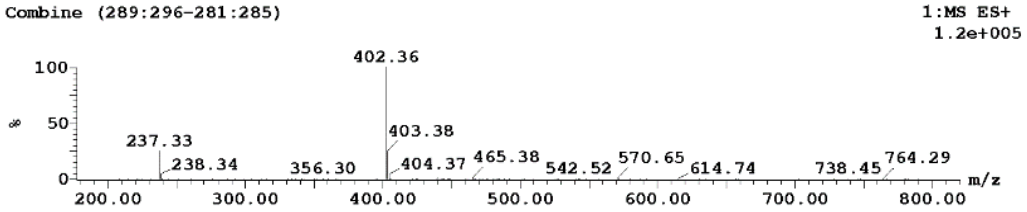


Compound **SC22**, $^{1}$H-NMR:

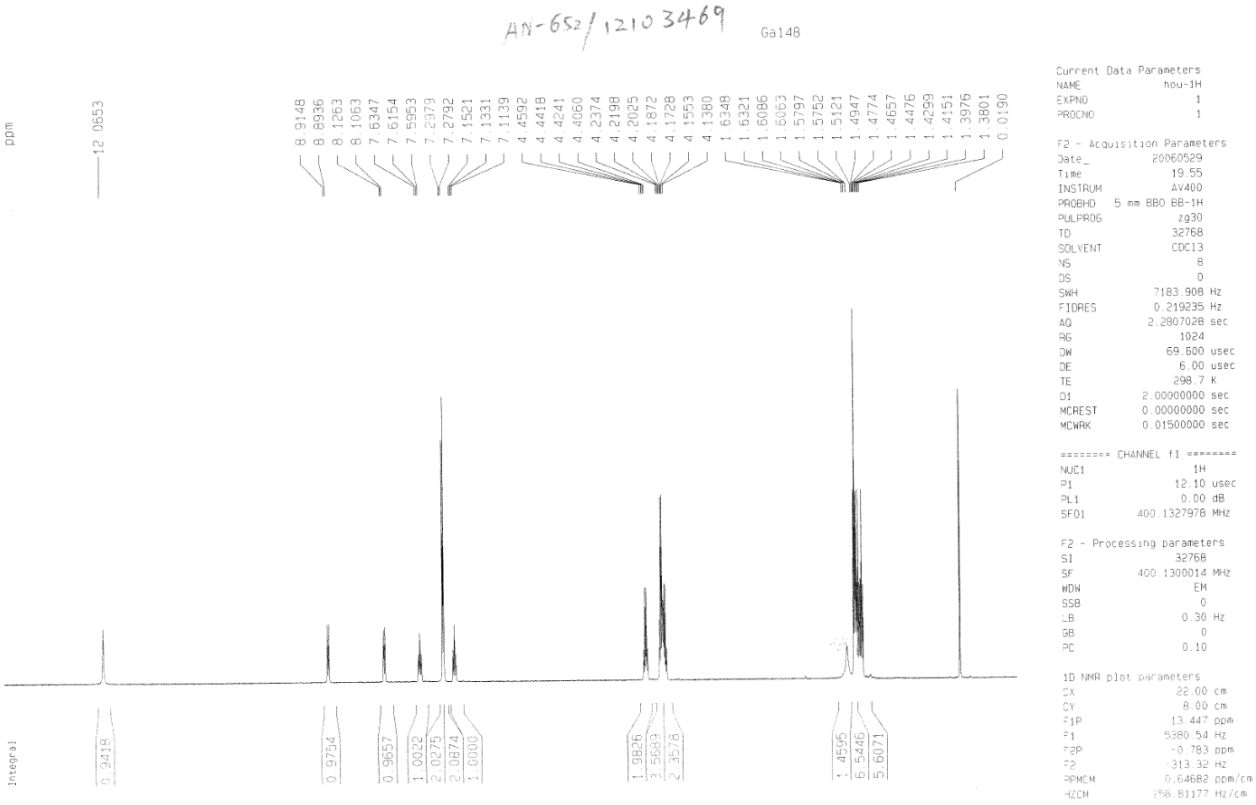


Compound **SC23**, LC-MS:

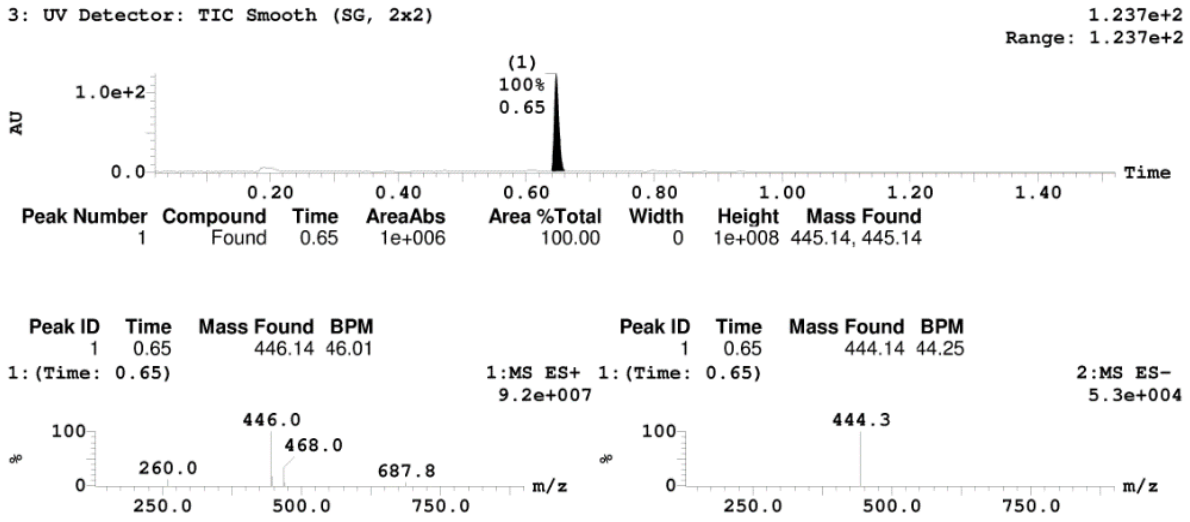


| Peak Number | Compound | Time | AreaAbs | Area %Total | Width | Height | Mass Found |
|---|---|---|---|---|---|---|---|
| 1 | Found | 0.65 | 1e+006 | 100.00 | 0 | 1e+008 | 445.14, 445.14 |

| Peak ID | Time | Mass Found | BPM |
|---|---|---|---|
| 1 | 0.65 | 446.14 | 46.01 |




| Peak ID | Time | Mass Found | BPM |
|---|---|---|---|
| 1 | 0.65 | 444.14 | 44.25 |




Compound **SC24**, LC-MS:

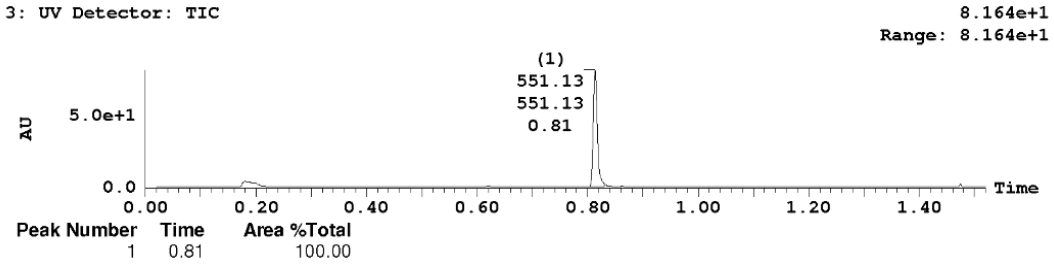


| Peak Number | Time | Area %Total |
|---|---|---|
| 1 | 0.81 | 100.00 |

| Peak ID | Time | Mass Found | BPM |
|---|---|---|---|
| 1 | 0.81 | 551.13 | 552.14 |

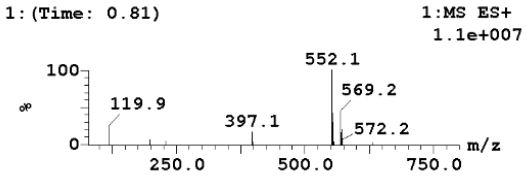


| Peak ID | Time | Mass Found | BPM |
|---|---|---|---|
| 1 | 0.81 | 551.13 | 550.29 |

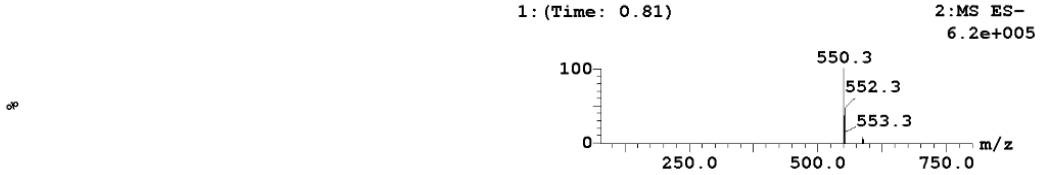


Compound **SC24**, $^{1}$H-NMR:

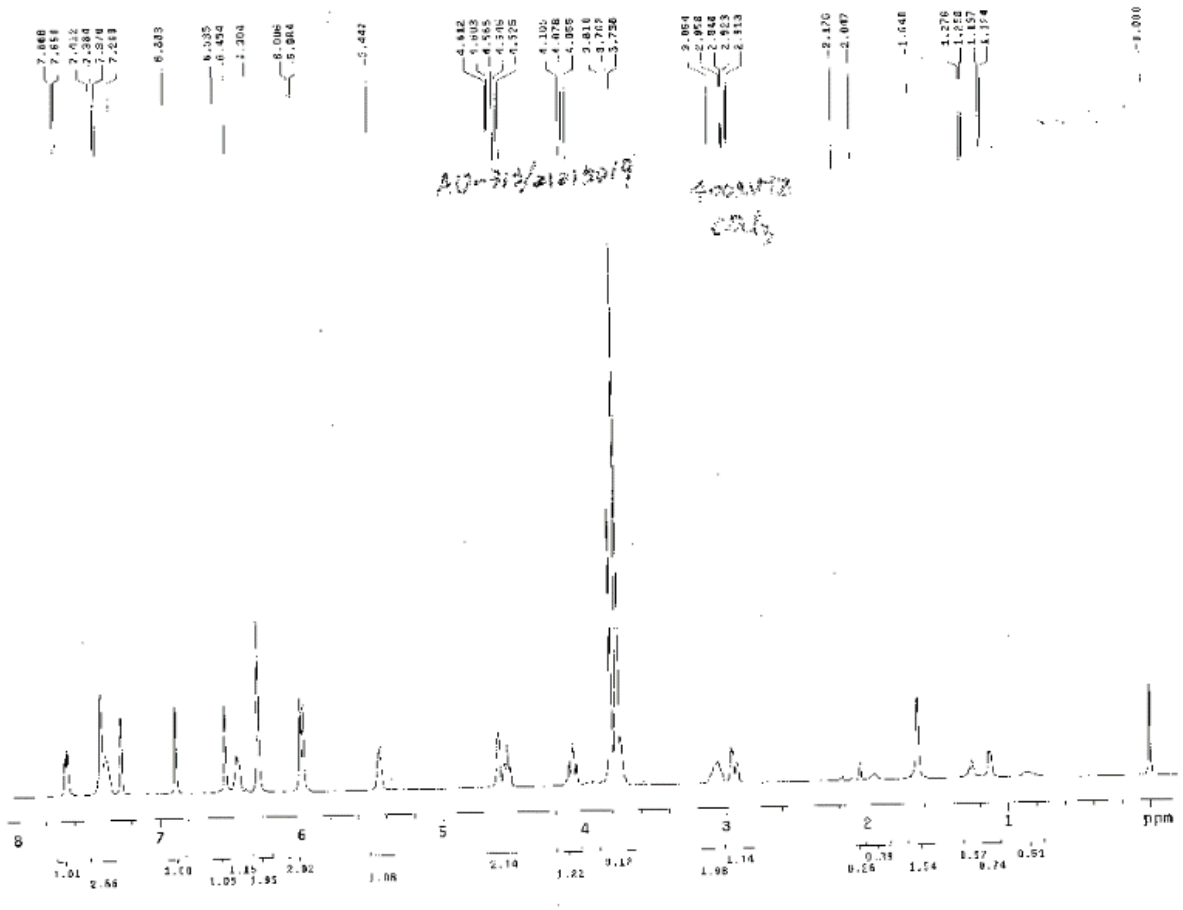

Compound **SC25**, LC-MS:

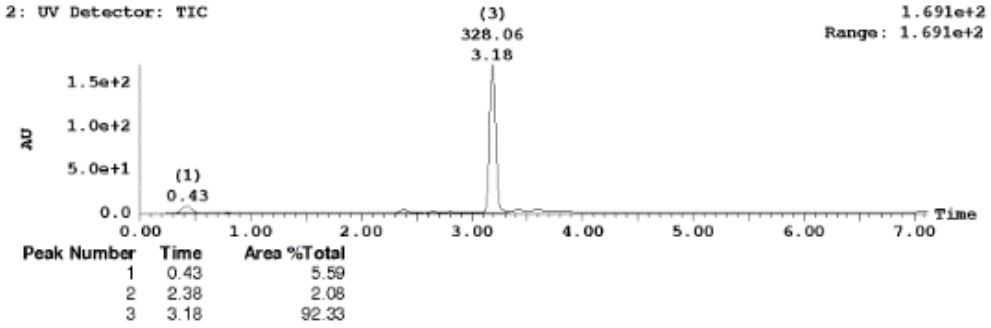


| Peak Number | Time | Area %Total |
|---|---|---|
| 1 | 0.43 | 5.59 |
| 2 | 2.38 | 2.08 |
| 3 | 3.18 | 92.33 |

| Peak ID | Time | Mass Found | BPM |
|---|---|---|---|
| 1 | 0.43 | | 257.20 |

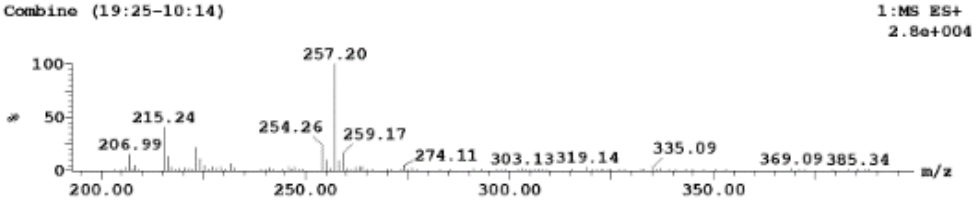


| Peak ID | Time | Mass Found | BPM |
|---|---|---|---|
| 2 | 2.38 | | 395.15 |

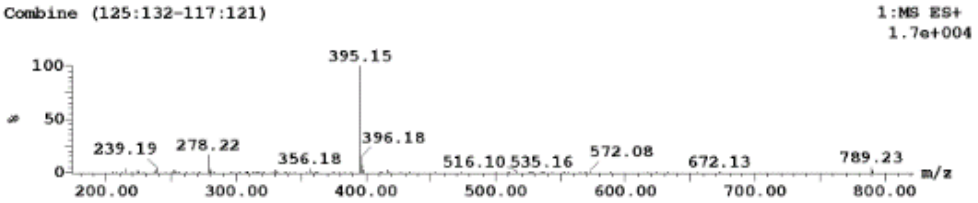


| Peak ID | Time | Mass Found | BPM |
|---|---|---|---|
| 3 | 3.18 | 328.06 | 329.20 |

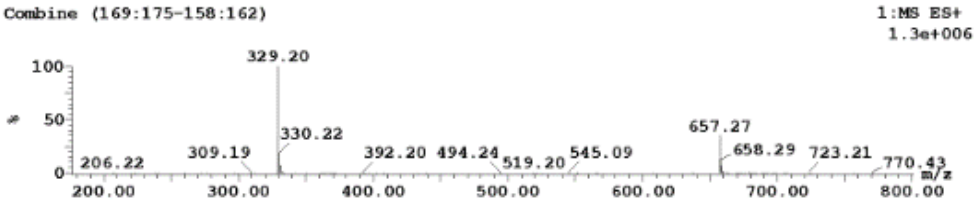


Compound **SC27**, LC-MS:

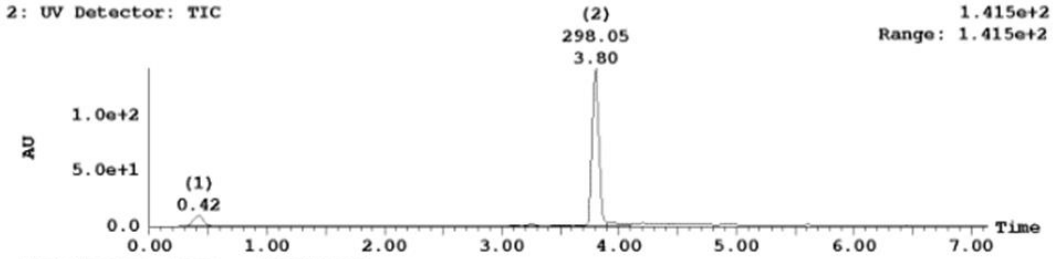


| Peak Number | Time | Area %Total |
|---|---|---|
| 1 | 0.42 | 7.91 |
| 2 | 3.80 | 89.89 |
| 3 | 3.95 | 2.20 |

| Peak ID | Time | Mass Found | BPM |
|---|---|---|---|
| 1 | 0.42 | | 223.23 |

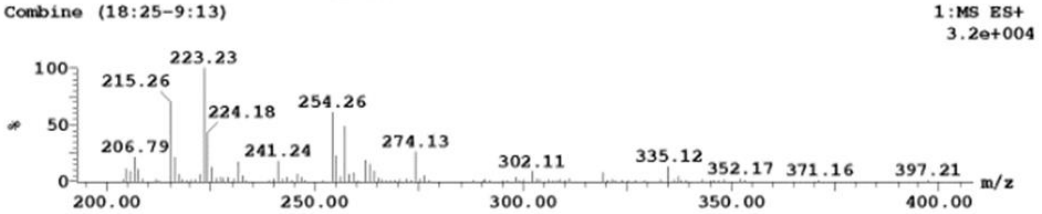


| Peak ID | Time | Mass Found | BPM |
|---|---|---|---|
| 2 | 3.80 | 298.05 | 299.24 |

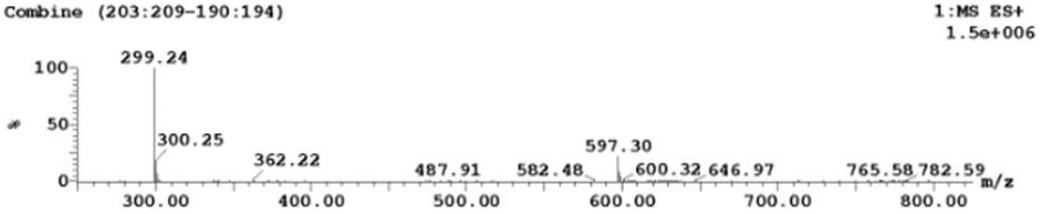


| Peak ID | Time | Mass Found | BPM |
|---|---|---|---|
| 3 | 3.95 | | 613.30 |

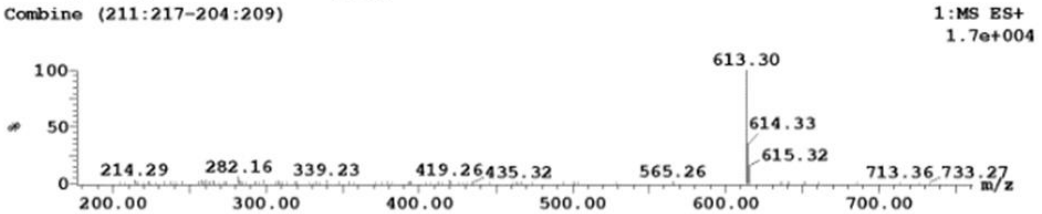


Compound **SC27**, $^{1}$H-NMR:

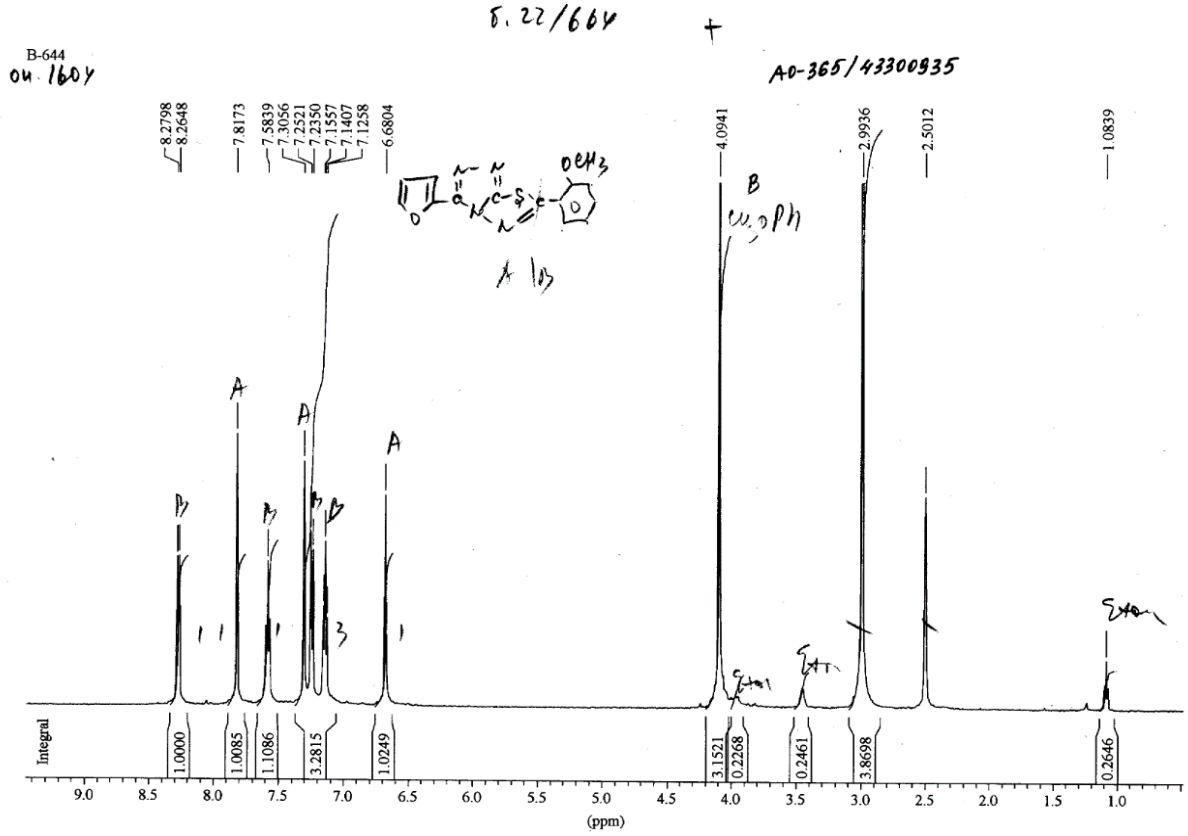


Compound **SC32**, LC-MS:

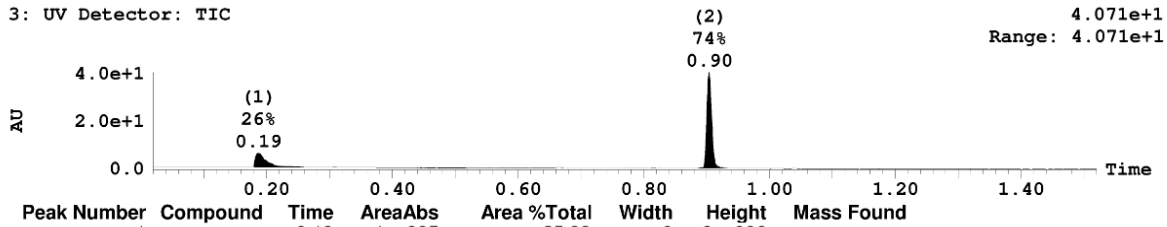


| Peak Number | Compound | Time | AreaAbs | Area %Total | Width | Height | Mass Found |
|---|---|---|---|---|---|---|---|
| 1 | | 0.19 | 1e+005 | 25.93 | 0 | 6e+006 | |
| 2 | Found | 0.90 | 4e+005 | 74.07 | 0 | 4e+007 | 446.88 |

| Peak ID | Time | Mass Found | BPM |
|---|---|---|---|
| 1 | 0.19 | | 45.86 |

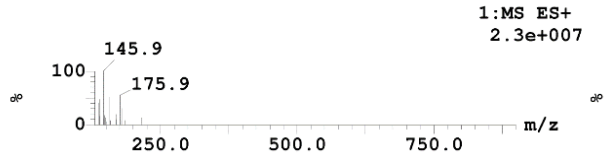


| Peak ID | Time | Mass Found | BPM |
|---|---|---|---|
| 2 | 0.90 | 447.88 | 49.76 |

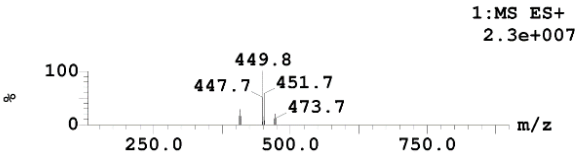


Compound **SC34**, LC-MS:

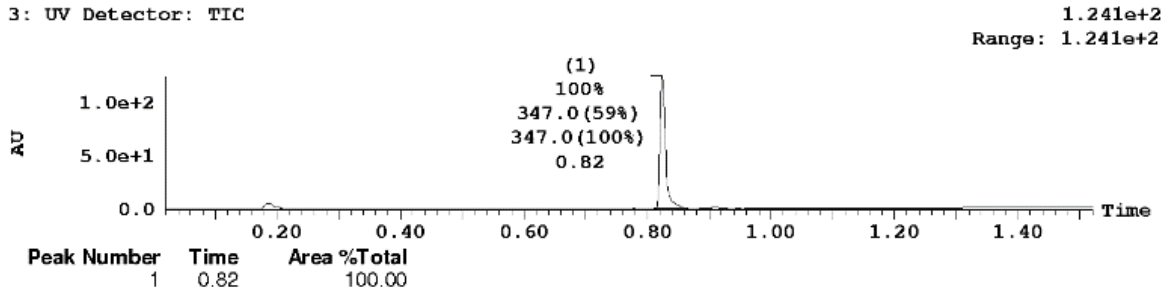


| Peak Number | Time | Area %Total |
|---|---|---|
| 1 | 0.82 | 100.00 |

| Peak ID | Time | Mass Found | BPM |
|---|---|---|---|
| 1 | 0.82 | 346.98 | 348.27 |

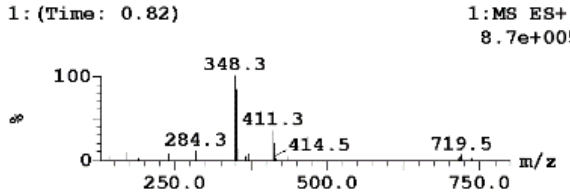


| Peak ID | Time | Mass Found | BPM |
|---|---|---|---|
| 1 | 0.82 | 346.98 | 346.24 |

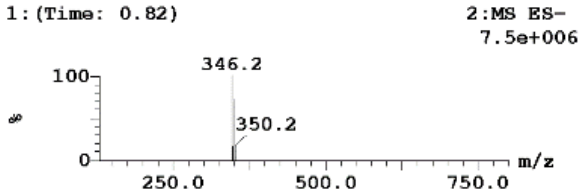


Compound **SC37**, $^{1}$H-NMR:

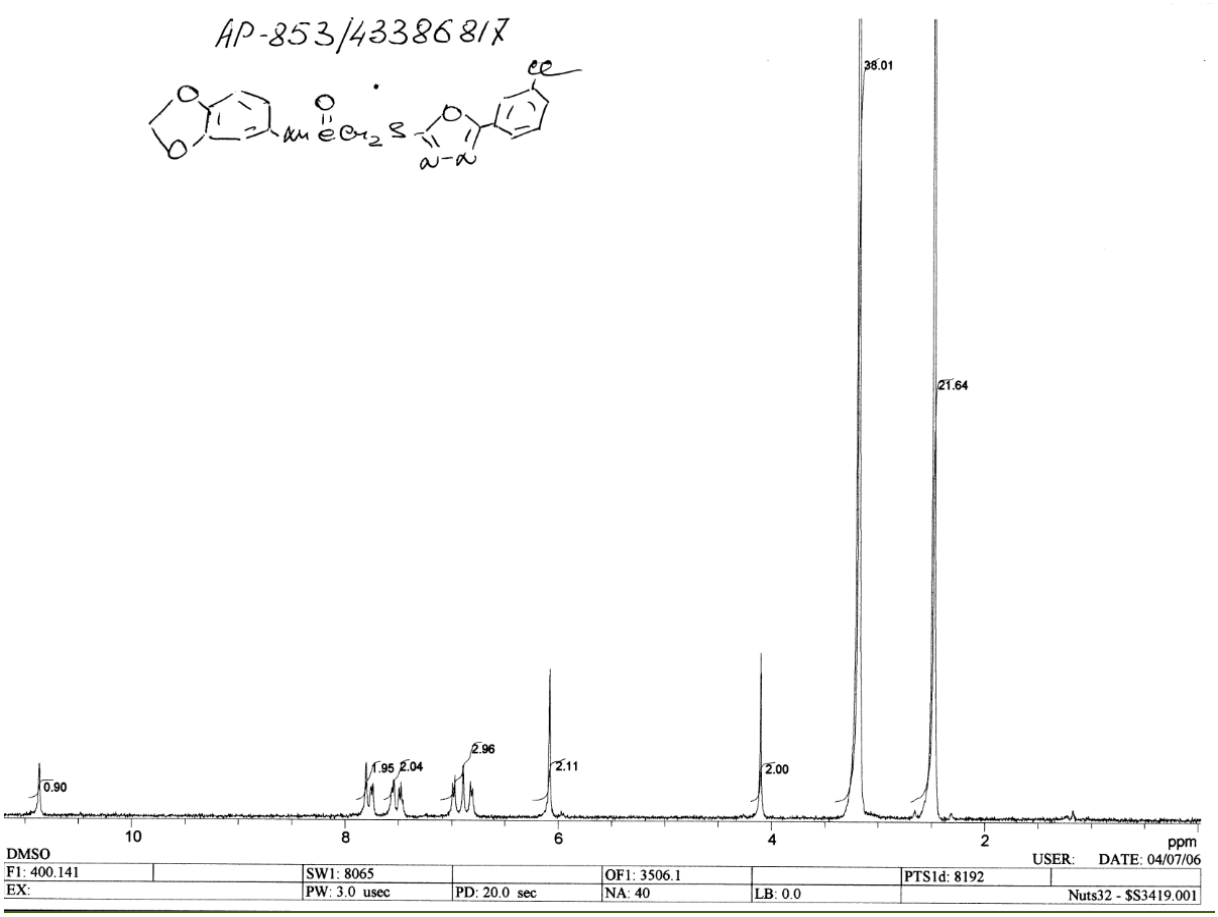


Compound **SC45**, LC-MS:

**Sample Report (continued):**

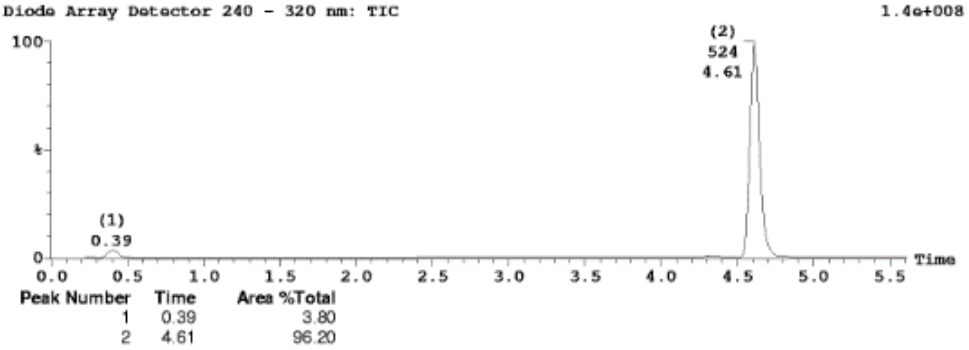


| Peak Number | Time | Area %Total |
|---|---|---|
| 1 | 0.39 | 3.80 |
| 2 | 4.61 | 96.20 |

| Peak ID | Time | Mass Found | BPM |
|---|---|---|---|
| 1 | 0.39 | | 215 |

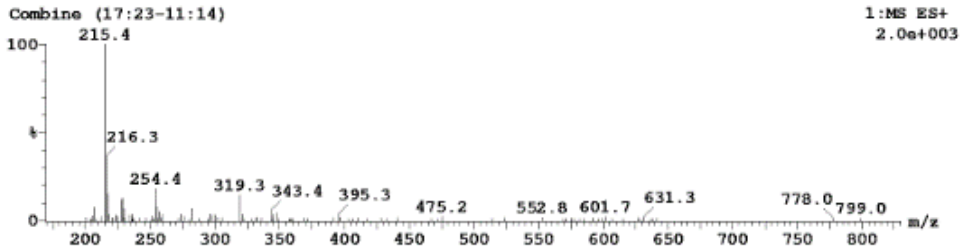


| Peak ID | Time | Mass Found | BPM |
|---|---|---|---|
| 2 | 4.61 | 524.08 | 525 |

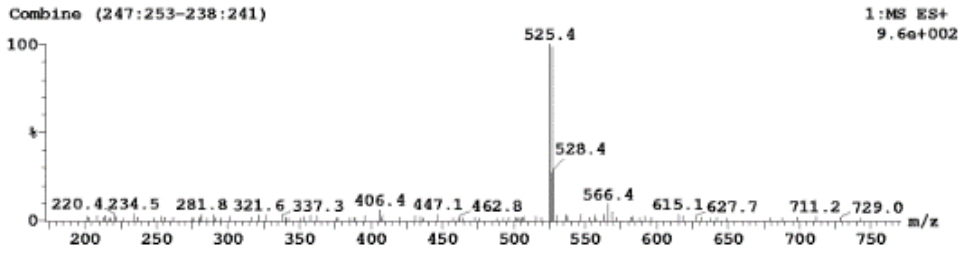

Compound **SC45**, $^{1}$H-NMR:

A

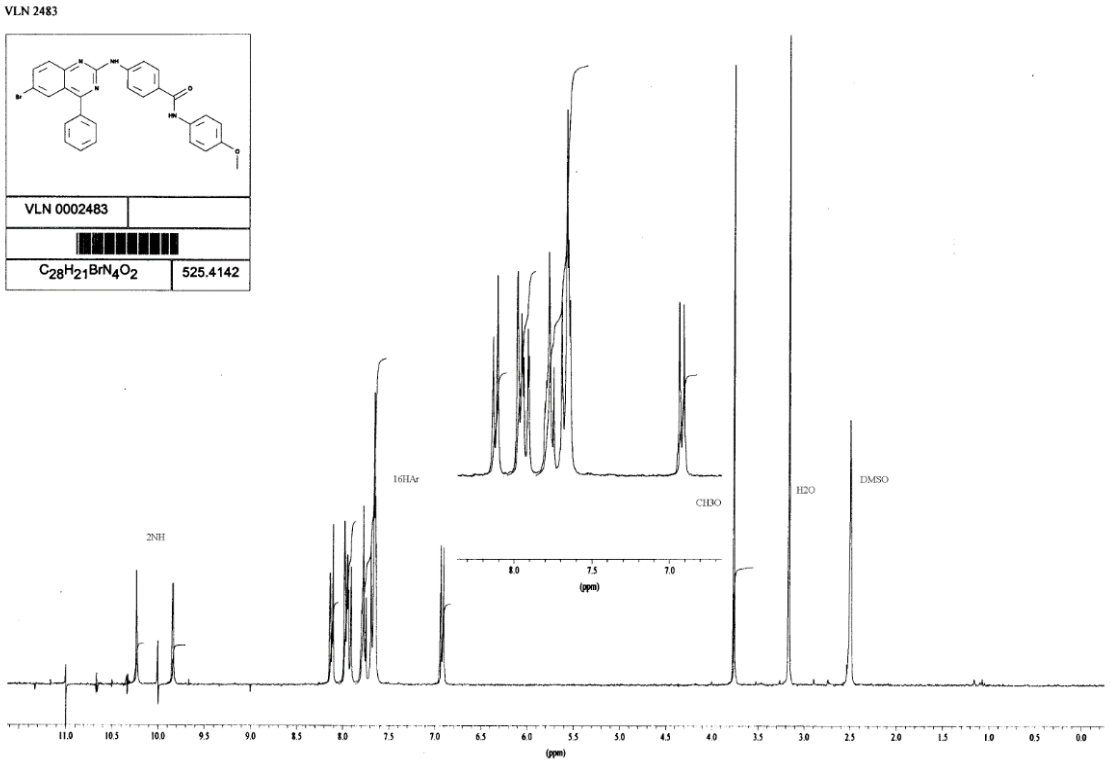

## References


1. Zhou, Y.; Xu, J.; Zhu, Y.; Duan, Y.; Zhou, M. Mechanism of Action of the Benzimidazole Fungicide on Fusarium graminearum: Interfering with Polymerization of Monomeric Tubulin But Not Polymerized Microtubule. *Phytopathology.* **2016,** *106*, 807-813. DOI: 10.1094/phyto-08-15-0186-r.

2. Lacey, E.; Brady, R. L.; Prichard, R. K.; Watson, T. R. Comparison of inhibition of polymerisation of mammalian tubulin and helminth ovicidal activity by benzimidazole carbamates. *Vet. Parasitol.* **1987,** *23*, 105-119. DOI: 10.1016/0304-4017(87)90029-X.

3. Morgan, U. M.; Reynoldson, J. A.; Thompson, R. C. Activities of several benzimidazoles and tubulin inhibitors against Giardia spp. in vitro. *Antimicrob. Agents Chemother.* **1993,** *37*, 328-31. DOI: 10.1128/aac.37.2.328.

4. Kamal, A.; Bharath Kumar, G.; Lakshma Nayak, V.; Reddy, V. S.; Shaik, A. B.; Rajender; Kashi Reddy, M. Design, synthesis and biological evaluation of imidazopyridine/imidazopyrimidine-benzimidazole conjugates as potential anticancer agents. *MedChemComm.* **2015,** *6*, 606-612. DOI: 10.1039/C4MD00400K.

5. Wu, Y.; Guan, Q.; Zheng, D.; Yan, P.; Feng, D.; Du, J.; Zhang, J.; Zuo, D.; Bao, K.; Zhang, W. Conformation impacts on the bioactivities of SMART analogues. *Eur. J. Med. Chem.* **2018,** *158*, 733-742. DOI: 10.1016/j.ejmech.2018.09.045.

6. Wang, F.; Yang, Z.; Liu, Y.; Ma, L.; Wu, Y.; He, L.; Shao, M.; Yu, K.; Wu, W.; Pu, Y.; Nie, C.; Chen, L. Synthesis and biological evaluation of diarylthiazole derivatives as antimitotic and antivascular agents with potent antitumor activity. *Bioorg. Med. Chem.* **2015,** *23*, 3337-3350. DOI: 10.1016/j.bmc.2015.04.055.

7. Zhang, Q.; Zhai, S.; Li, L.; Li, X.; Zhou, H.; Liu, A.; Su, G.; Mu, Q.; Du, Y.; Yan, B. Anti-tumor selectivity of a novel Tubulin and HSP90 dual-targeting inhibitor in non-small cell lung cancer models. *Biochem. Pharmacol.* **2013,** *86*, 351-360. DOI: 10.1016/j.bcp.2013.05.019.

8. Li, L.; Liu, Y.; Zhang, Q.; Zhou, H.; Zhang, Y.; Yan, B. Comparison of Cancer Cell Survival Triggered by Microtubule Damage after Turning Dyrk1B Kinase On and Off. *ACS Chem. Biol.* **2014,** *9*, 731-742. DOI: 10.1021/cb4005589.

9. Mu, Y.; Liu, Y.; Li, L.; Tian, C.; Zhou, H.; Zhang, Q.; Yan, B. The novel tubulin polymerization inhibitor MHPT exhibits selective anti-tumor activity against rhabdomyosarcoma in vitro and in vivo. *PLoS One.* **2015,** *10*, e0121806. DOI: 10.1371/journal.pone.0121806.

10. Lawrence, N. J.; Rennison, D.; McGown, A. T.; Ducki, S.; Gul, L. A.; Hadfield, J. A.; Khan, N. Linked Parallel Synthesis and MTT Bioassay Screening of Substituted Chalcones. *J. Comb. Chem.* **2001,** *3*, 421-426. DOI: 10.1021/cc000075z.

11. Woods, J. A.; Hadfield, J. A.; Pettit, G. R.; Fox, B. W.; McGown, A. T. The interaction with tubulin of a series of stilbenes based on combretastatin A-4. *Br. J. Cancer.* **1995,** *71*, 705-711. DOI: 10.1038/bjc.1995.138.

12. Qian, Y.; Ma, G.-Y.; Yang, Y.; Cheng, K.; Zheng, Q.-Z.; Mao, W.-J.; Shi, L.; Zhao, J.; Zhu, H.-L. Synthesis, molecular modeling and biological evaluation of dithiocarbamates as novel antitubulin agents. *Bioorg. Med. Chem.* **2010,** *18*, 4310-4316. DOI: 10.1016/j.bmc.2010.04.091.

13. Salum, L. B.; Altei, W. F.; Chiaradia, L. D.; Cordeiro, M. N. S.; Canevarolo, R. R.; Melo, C. P. S.; Winter, E.; Mattei, B.; Daghestani, H. N.; Santos-Silva, M. C.; Creczynski-

Pasa, T. B.; Yunes, R. A.; Yunes, J. A.; Andricopulo, A. D.; Day, B. W.; Nunes, R. J.; Vogt, A. Cytotoxic 3,4,5-trimethoxychalcones as mitotic arresters and cell migration inhibitors. *Eur. J. Med. Chem.* **2013,** *63*, 501-510. DOI: 10.1016/j.ejmech.2013.02.037.

14. Wang, Y.-T.; Qin, Y.-J.; Zhang, Y.-L.; Li, Y.-J.; Rao, B.; Zhang, Y.-Q.; Yang, M.-R.; Jiang, A.-Q.; Qi, J.-L.; Zhu, H.-L. Synthesis, biological evaluation, and molecular docking studies of novel chalcone oxime derivatives as potential tubulin polymerization inhibitors. *RSC Adv.* **2014,** *4*, 32263-32275. DOI: 10.1039/C4RA03803G.

15. Zhu, C.; Zuo, Y.; Wang, R.; Liang, B.; Yue, X.; Wen, G.; Shang, N.; Huang, L.; Chen, Y.; Du, J.; Bu, X. Discovery of Potent Cytotoxic Ortho-Aryl Chalcones as New Scaffold Targeting Tubulin and Mitosis with Affinity-Based Fluorescence. *J. Med. Chem.* **2014,** *57*, 6364-6382. DOI: 10.1021/jm500024v.

16. Chen, J.; Yan, J.; Hu, J.; Pang, Y.; Huang, L.; Li, X. Synthesis, biological evaluation and mechanism study of chalcone analogues as novel anti-cancer agents. *RSC Adv.* **2015,** *5*, 68128-68135. DOI: 10.1039/C5RA14888J.

17. Yan, J.; Chen, J.; Zhang, S.; Hu, J.; Huang, L.; Li, X. Synthesis, Evaluation, and Mechanism Study of Novel Indole-Chalcone Derivatives Exerting Effective Antitumor Activity Through Microtubule Destabilization in Vitro and in Vivo. *J. Med. Chem.* **2016,** *59*, 5264-5283. DOI: 10.1021/acs.jmedchem.6b00021.

18. Ducki, S.; Rennison, D.; Woo, M.; Kendall, A.; Chabert, J. F. D.; McGown, A. T.; Lawrence, N. J. Combretastatin-like chalcones as inhibitors of microtubule polymerization. Part 1: Synthesis and biological evaluation of antivascular activity. *Bioorg. Med. Chem.* **2009,** *17*, 7698-7710. DOI: 10.1016/j.bmc.2009.09.039.

19. Ducki, S.; Mackenzie, G.; Lawrence, N. J.; Snyder, J. P. Quantitative Structure−Activity Relationship (5D-QSAR) Study of Combretastatin-like Analogues as Inhibitors of Tubulin Assembly. *J. Med. Chem.* **2005,** *48*, 457-465. DOI: 10.1021/jm049444m.

20. Thomopoulou, P.; Sachs, J.; Teusch, N.; Mariappan, A.; Gopalakrishnan, J.; Schmalz, H.-G. New Colchicine-Derived Triazoles and Their Influence on Cytotoxicity and Microtubule Morphology. *ACS Med. Chem. Lett.* **2016,** *7*, 188-191. DOI: 10.1021/acsmedchemlett.5b00418.

21. Cifuentes, M.; Schilling, B.; Ravindra, R.; Winter, J.; Janik, M. E. Synthesis and biological evaluation of B-ring modified colchicine and isocolchicine analogs. *Bioorg. Med. Chem. Lett.* **2006,** *16*, 2761-2764. DOI: 10.1016/j.bmcl.2006.02.010.

22. Cosentino, L.; Redondo-Horcajo, M.; Zhao, Y.; Santos, A. R.; Chowdury, K. F.; Vinader, V.; Abdallah, Q. M. A.; Abdel-Rahman, H.; Fournier-Dit-Chabert, J.; Shnyder, S. D.; Loadman, P. M.; Fang, W.-s.; Díaz, J. F.; Barasoain, I.; Burns, P. A.; Pors, K. Synthesis and Biological Evaluation of Colchicine B-Ring Analogues Tethered with Halogenated Benzyl Moieties. *J. Med. Chem.* **2012,** *55*, 11062-11066. DOI: 10.1021/jm301151t.

23. Singh, B.; Kumar, A.; Joshi, P.; Guru, S. K.; Kumar, S.; Wani, Z. A.; Mahajan, G.; Hussain, A.; Qazi, A. K.; Kumar, A.; Bharate, S. S.; Gupta, B. D.; Sharma, P. R.; Hamid, A.; Saxena, A. K.; Mondhe, D. M.; Bhushan, S.; Bharate, S. B.; Vishwakarma, R. A. Colchicine derivatives with potent anticancer activity and reduced P-glycoprotein induction liability. *Org. Biomol. Chem.* **2015,** *13*, 5674-5689. DOI: 10.1039/C5OB00406C.

24. Romagnoli, R.; Baraldi, P. G.; Salvador, M. K.; Preti, D.; Aghazadeh Tabrizi, M.; Brancale, A.; Fu, X.-H.; Li, J.; Zhang, S.-Z.; Hamel, E.; Bortolozzi, R.; Basso, G.; Viola, G. Synthesis and Evaluation of 1,5-Disubstituted Tetrazoles as Rigid Analogues of

Combretastatin A-4 with Potent Antiproliferative and Antitumor Activity. *J. Med. Chem.* **2012,** *55*, 475-488. DOI: 10.1021/jm2013979.

25. Flynn, B. L.; Gill, G. S.; Grobelny, D. W.; Chaplin, J. H.; Paul, D.; Leske, A. F.; Lavranos, T. C.; Chalmers, D. K.; Charman, S. A.; Kostewicz, E.; Shackleford, D. M.; Morizzi, J.; Hamel, E.; Jung, M. K.; Kremmidiotis, G. Discovery of 7-Hydroxy-6-methoxy-2-methyl-3-(3,4,5-trimethoxybenzoyl)benzo[b]furan (BNC105), a Tubulin Polymerization Inhibitor with Potent Antiproliferative and Tumor Vascular Disrupting Properties. *J. Med. Chem.* **2011,** *54*, 6014-6027. DOI: 10.1021/jm200454y.

26. Sanghai, N.; Jain, V.; Preet, R.; Kandekar, S.; Das, S.; Trivedi, N.; Mohapatra, P.; Priyadarshani, G.; Kashyap, M.; Das, D.; Satapathy, S. R.; Siddharth, S.; Guchhait, S. K.; Kundu, C. N.; Bharatam, P. V. Combretastatin A-4 inspired novel 2-aryl-3-arylamino-imidazo-pyridines/pyrazines as tubulin polymerization inhibitors, antimitotic and anticancer agents. *MedChemComm.* **2014,** *5*, 766-782. DOI: 10.1039/C3MD00357D.

27. Yan, J.; Pang, Y.; Chen, J.; Sheng, J.; Hu, J.; Huang, L.; Li, X. Synthesis, biological evaluation and mechanism study of a class of cyclic combretastatin A-4 analogues as novel antitumour agents. *RSC Adv.* **2015,** *5*, 98527-98537. DOI: 10.1039/C5RA19270F.

28. De Martino, G.; La Regina, G.; Coluccia, A.; Edler, M. C.; Barbera, M. C.; Brancale, A.; Wilcox, E.; Hamel, E.; Artico, M.; Silvestri, R. Arylthioindoles, Potent Inhibitors of Tubulin Polymerization. *J. Med. Chem.* **2004,** *47*, 6120-6123. DOI: 10.1021/jm049360d.

29. De Martino, G.; Edler, M. C.; La Regina, G.; Coluccia, A.; Barbera, M. C.; Barrow, D.; Nicholson, R. I.; Chiosis, G.; Brancale, A.; Hamel, E.; Artico, M.; Silvestri, R. New Arylthioindoles: Potent Inhibitors of Tubulin Polymerization. 2. Structure−Activity

Relationships and Molecular Modeling Studies. *J. Med. Chem.* **2006,** *49*, 947-954. DOI: 10.1021/jm050809s.

30. La Regina, G.; Sarkar, T.; Bai, R.; Edler, M. C.; Saletti, R.; Coluccia, A.; Piscitelli, F.; Minelli, L.; Gatti, V.; Mazzoccoli, C.; Palermo, V.; Mazzoni, C.; Falcone, C.; Scovassi, A. I.; Giansanti, V.; Campiglia, P.; Porta, A.; Maresca, B.; Hamel, E.; Brancale, A.; Novellino, E.; Silvestri, R. New Arylthioindoles and Related Bioisosteres at the Sulfur Bridging Group. 4. Synthesis, Tubulin Polymerization, Cell Growth Inhibition, and Molecular Modeling Studies. *J. Med. Chem.* **2009,** *52*, 7512-7527. DOI: 10.1021/jm900016t.

31. Colley, H. E.; Muthana, M.; Danson, S. J.; Jackson, L. V.; Brett, M. L.; Harrison, J.; Coole, S. F.; Mason, D. P.; Jennings, L. R.; Wong, M.; Tulasi, V.; Norman, D.; Lockey, P. M.; Williams, L.; Dossetter, A. G.; Griffen, E. J.; Thompson, M. J. An Orally Bioavailable, Indole-3-glyoxylamide Based Series of Tubulin Polymerization Inhibitors Showing Tumor Growth Inhibition in a Mouse Xenograft Model of Head and Neck Cancer. *J. Med. Chem.* **2015,** *58*, 9309-9333. DOI: 10.1021/acs.jmedchem.5b01312.

32. Wen, Z.; Xu, J.; Wang, Z.; Qi, H.; Xu, Q.; Bai, Z.; Zhang, Q.; Bao, K.; Wu, Y.; Zhang, W. 3-(3,4,5-Trimethoxyphenylselenyl)-1H-indoles and their selenoxides as combretastatin A-4 analogs: Microwave-assisted synthesis and biological evaluation. *Eur. J. Med. Chem.* **2015,** *90*, 184-194. DOI: 10.1016/j.ejmech.2014.11.024.

33. Diao, P. C.; Li, Q.; Hu, M.-J.; Ma, Y.-F.; You, W.-W.; Hong, K. H.; Zhao, P.-L. Synthesis and biological evaluation of novel indole-pyrimidine hybrids bearing morpholine and thiomorpholine moieties. *Eur. J. Med. Chem.* **2017,** *134*, 110-118. DOI: 10.1016/j.ejmech.2017.04.011.

34. La Regina, G.; Bai, R.; Rensen, W.; Coluccia, A.; Piscitelli, F.; Gatti, V.; Bolognesi, A.; Lavecchia, A.; Granata, I.; Porta, A.; Maresca, B.; Soriani, A.; Iannitto, M. L.; Mariani, M.; Santoni, A.; Brancale, A.; Ferlini, C.; Dondio, G.; Varasi, M.; Mercurio, C.; Hamel, E.; Lavia, P.; Novellino, E.; Silvestri, R. Design and Synthesis of 2-Heterocyclyl-3-arylthio-1H-indoles as Potent Tubulin Polymerization and Cell Growth Inhibitors with Improved Metabolic Stability. *J. Med. Chem.* **2011,** *54*, 8394-8406. DOI: 10.1021/jm2012886.

35. La Regina, G.; Bai, R.; Rensen, W. M.; Di Cesare, E.; Coluccia, A.; Piscitelli, F.; Famiglini, V.; Reggio, A.; Nalli, M.; Pelliccia, S.; Da Pozzo, E.; Costa, B.; Granata, I.; Porta, A.; Maresca, B.; Soriani, A.; Iannitto, M. L.; Santoni, A.; Li, J.; Miranda Cona, M.; Chen, F.; Ni, Y.; Brancale, A.; Dondio, G.; Vultaggio, S.; Varasi, M.; Mercurio, C.; Martini, C.; Hamel, E.; Lavia, P.; Novellino, E.; Silvestri, R. Toward Highly Potent Cancer Agents by Modulating the C-2 Group of the Arylthioindole Class of Tubulin Polymerization Inhibitors. *J. Med. Chem.* **2013,** *56*, 123-149. DOI: 10.1021/jm3013097.

36. La Regina, G.; Bai, R.; Coluccia, A.; Famiglini, V.; Pelliccia, S.; Passacantilli, S.; Mazzoccoli, C.; Ruggieri, V.; Verrico, A.; Miele, A.; Monti, L.; Nalli, M.; Alfonsi, R.; Di Marcotullio, L.; Gulino, A.; Ricci, B.; Soriani, A.; Santoni, A.; Caraglia, M.; Porto, S.; Da Pozzo, E.; Martini, C.; Brancale, A.; Marinelli, L.; Novellino, E.; Vultaggio, S.; Varasi, M.; Mercurio, C.; Bigogno, C.; Dondio, G.; Hamel, E.; Lavia, P.; Silvestri, R. New Indole Tubulin Assembly Inhibitors Cause Stable Arrest of Mitotic Progression, Enhanced Stimulation of Natural Killer Cell Cytotoxic Activity, and Repression of Hedgehog-Dependent Cancer. *J. Med. Chem.* **2015,** *58*, 5789-5807. DOI: 10.1021/acs.jmedchem.5b00310.

37. MacDonough, M. T.; Strecker, T. E.; Hamel, E.; Hall, J. J.; Chaplin, D. J.; Trawick, M. L.; Pinney, K. G. Synthesis and biological evaluation of indole-based, anti-cancer agents inspired by the vascular disrupting agent 2-(3′-hydroxy-4′-methoxyphenyl)-3-(3″,4″,5″-

trimethoxybenzoyl)-6-methoxyindole (OXi8006). *Bioorg. Med. Chem.* **2013,** *21*, 6831-6843. DOI: 10.1016/j.bmc.2013.07.028.

38. Owa, T.; Yokoi, A.; Yamazaki, K.; Yoshimatsu, K.; Yamori, T.; Nagasu, T. Array-Based Structure and Gene Expression Relationship Study of Antitumor Sulfonamides Including N-[2-[(4-Hydroxyphenyl)amino]-3-pyridinyl]-4-methoxybenzenesulfonamide and N-(3-Chloro-7-indolyl)-1,4-benzenedisulfonamide. *J. Med. Chem.* **2002,** *45*, 4913-4922. DOI: 10.1021/jm0201060.

39. Owa, T.; Okauchi, T.; Yoshimatsu, K.; Sugi, N. H.; Ozawa, Y.; Nagasu, T.; Koyanagi, N.; Okabe, T.; Kitoh, K.; Yoshino, H. A focused compound library of novel N-(7-indolyl)benzenesulfonamides for the discovery of potent cell cycle inhibitors. *Bioorg. Med. Chem. Lett.* **2000,** *10*, 1223-1226. DOI: 10.1016/S0960-894X(00)00219-5.

40. Yokoi, A.; Kuromitsu, J.; Kawai, T.; Nagasu, T.; Hata Sugi, N.; Yoshimatsu, K.; Yoshino, H.; Owa, T. Profiling Novel Sulfonamide Antitumor Agents with Cell-based Phenotypic Screens and Array-based Gene Expression Analysis. *Mol. Cancer. Ther.* **2002,** *1*, 275-286.

41. Chang, J.-Y.; Hsieh, H.-P.; Chang, C.-Y.; Hsu, K.-S.; Chiang, Y.-F.; Chen, C.-M.; Kuo, C.-C.; Liou, J.-P. 7-Aroyl-aminoindoline-1-sulfonamides as a Novel Class of Potent Antitubulin Agents. *J. Med. Chem.* **2006,** *49*, 6656-6659. DOI: 10.1021/jm061076u.

42. Wang, Y.-M.; Hu, L.-X.; Liu, Z.-M.; You, X.-F.; Zhang, S.-H.; Qu, J.-R.; Li, Z.-R.; Li, Y.; Kong, W.-J.; He, H.-W.; Shao, R.-G.; Zhang, L.-R.; Peng, Z.-G.; Boykin, D. W.; Jiang, J.-D. N-(2,6-Dimethoxypyridine-3-yl)-9-Methylcarbazole-3-Sulfonamide as a Novel Tubulin Ligand against Human Cancer. *Clin. Cancer. Res.* **2008,** *14*, 6218-6227. DOI: 10.1158/1078-0432.Ccr-08-0550.

43. Shan, B.; Medina, J. C.; Santha, E.; Frankmoelle, W. P.; Chou, T. C.; Learned, R. M.; Narbut, M. R.; Stott, D.; Wu, P.; Jaen, J. C.; Rosen, T.; Timmermans, P. B.; Beckmann, H. Selective, covalent modification of beta-tubulin residue Cys-239 by T138067, an antitumor agent with in vivo efficacy against multidrug-resistant tumors. *Proc. Natl. Acad. Sci. U.S.A.* **1999,** *96*, 5686-91. DOI: 10.1073/pnas.96.10.5686.

44. Reddy, M. V. R.; Mallireddigari, M. R.; Pallela, V. R.; Cosenza, S. C.; Billa, V. K.; Akula, B.; Subbaiah, D. R. C. V.; Bharathi, E. V.; Padgaonkar, A.; Lv, H.; Gallo, J. M.; Reddy, E. P. Design, Synthesis, and Biological Evaluation of (E)-N-Aryl-2-arylethenesulfonamide Analogues as Potent and Orally Bioavailable Microtubule-Targeted Anticancer Agents. *J. Med. Chem.* **2013,** *56*, 5562-5586. DOI: 10.1021/jm400575x.

45. Popowycz, F.; Schneider, C.; DeBonis, S.; Skoufias, D. A.; Kozielski, F.; Galmarini, C. M.; Joseph, B. Synthesis and antiproliferative evaluation of pyrazolo[1,5-a]-1,3,5-triazine myoseverin derivatives. *Bioorg. Med. Chem.* **2009,** *17*, 3471-3478. DOI: 10.1016/j.bmc.2009.03.007.

46. Moon, H.-S.; Jacobson, E. M.; Khersonsky, S. M.; Luzung, M. R.; Walsh, D. P.; Xiong, W.; Lee, J. W.; Parikh, P. B.; Lam, J. C.; Kang, T.-W.; Rosania, G. R.; Schier, A. F.; Chang, Y.-T. A Novel Microtubule Destabilizing Entity from Orthogonal Synthesis of Triazine Library and Zebrafish Embryo Screening. *J. Am. Chem. Soc.* **2002,** *124*, 11608-11609. DOI: 10.1021/ja026720i.

47. Chang, Y.-T.; Wignall, S. M.; Rosania, G. R.; Gray, N. S.; Hanson, S. R.; Su, A. I.; Merlie, J.; Moon, H.-S.; Sangankar, S. B.; Perez, O.; Heald, R.; Schultz, P. G. Synthesis and Biological Evaluation of Myoseverin Derivatives: Microtubule Assembly Inhibitors. *J. Med. Chem.* **2001,** *44*, 4497-4500. DOI: 10.1021/jm010451+.

48. Kryštof, V.; Moravcová, D.; Paprskářová, M.; Barbier, P.; Peyrot, V.; Hlobilková, A.; Havlíček, L.; Strnad, M. Synthesis and biological activity of 8-azapurine and pyrazolo[4,3-d]pyrimidine analogues of myoseverin. *Eur. J. Med. Chem.* **2006,** *41*, 1405-1411. DOI: 10.1016/j.ejmech.2006.07.004.

49. Kuo, S. C.; Lee, H. Z.; Juang, J. P.; Lin, Y. T.; Wu, T. S.; Chang, J. J.; Lednicer, D.; Paull, K. D.; Lin, C. M. Synthesis and cytotoxicity of 1,6,7,8-substituted 2-(4'-substituted phenyl)-4-quinolones and related compounds: identification as antimitotic agents interacting with tubulin. *J. Med. Chem.* **1993,** *36*, 1146-1156. DOI: 10.1021/jm00061a005.

50. Abad, A.; López-Pérez, J. L.; del Olmo, E.; García-Fernández, L. F.; Francesch, A.; Trigili, C.; Barasoain, I.; Andreu, J. M.; Díaz, J. F.; San Feliciano, A. Synthesis and Antimitotic and Tubulin Interaction Profiles of Novel Pinacol Derivatives of Podophyllotoxins. *J. Med. Chem.* **2012,** *55*, 6724-6737. DOI: 10.1021/jm2017573.

51. Labruère, R.; Gautier, B.; Testud, M.; Seguin, J.; Lenoir, C.; Desbène-Finck, S.; Helissey, P.; Garbay, C.; Chabot, G. G.; Vidal, M.; Giorgi-Renault, S. Design, Synthesis, and Biological Evaluation of the First Podophyllotoxin Analogues as Potential Vascular-Disrupting Agents. *ChemMedChem.* **2010,** *5*, 2016-2025. DOI: 10.1002/cmdc.201000305.

52. Prinz, H.; Ishii, Y.; Hirano, T.; Stoiber, T.; Camacho Gomez, J. A.; Schmidt, P.; Düssmann, H.; Burger, A. M.; Prehn, J. H. M.; Günther, E. G.; Unger, E.; Umezawa, K. Novel Benzylidene-9(10H)-anthracenones as Highly Active Antimicrotubule Agents. Synthesis, Antiproliferative Activity, and Inhibition of Tubulin Polymerization. *J. Med. Chem.* **2003,** *46*, 3382-3394. DOI: 10.1021/jm0307685.

53. Zuse, A.; Schmidt, P.; Baasner, S.; Böhm, K. J.; Müller, K.; Gerlach, M.; Günther, E. G.; Unger, E.; Prinz, H. Sulfonate Derivatives of Naphtho[2,3-b]thiophen-4(9H)-one and

9(10H)-Anthracenone as Highly Active Antimicrotubule Agents. Synthesis, Antiproliferative Activity, and Inhibition of Tubulin Polymerization. *J. Med. Chem.* **2007,** *50*, 6059-6066. DOI: 10.1021/jm0708984.

54. Prinz, H.; Schmidt, P.; Böhm, K. J.; Baasner, S.; Müller, K.; Unger, E.; Gerlach, M.; Günther, E. G. 10-(2-oxo-2-Phenylethylidene)-10H-anthracen-9-ones as Highly Active Antimicrotubule Agents: Synthesis, Antiproliferative Activity, and Inhibition of Tubulin Polymerization. *J. Med. Chem.* **2009,** *52*, 1284-1294. DOI: 10.1021/jm801338r.

55. Surkau, G.; Böhm, K. J.; Müller, K.; Prinz, H. Synthesis, antiproliferative activity and inhibition of tubulin polymerization by anthracenone-based oxime derivatives. *Eur. J. Med. Chem.* **2010,** *45*, 3354-3364. DOI: 10.1016/j.ejmech.2010.04.019.

56. Prinz, H.; Schmidt, P.; Böhm, K. J.; Baasner, S.; Müller, K.; Gerlach, M.; Günther, E. G.; Unger, E. Phenylimino-10H-anthracen-9-ones as novel antimicrotubule agents—synthesis, antiproliferative activity and inhibition of tubulin polymerization. *Bioorg. Med. Chem.* **2011,** *19*, 4183-4191. DOI: 10.1016/j.bmc.2011.06.010.

57. Silva-García, E. M.; Cerda-García-Rojas, C. M.; del Río, R. E.; Joseph-Nathan, P. Parvifoline Derivatives as Tubulin Polymerization Inhibitors. *J. Nat. Prod.* **2019,** *82*, 840-849. DOI: 10.1021/acs.jnatprod.8b00860.

58. Wang, Y.; Zhang, H.; Gigant, B.; Yu, Y.; Wu, Y.; Chen, X.; Lai, Q.; Yang, Z.; Chen, Q.; Yang, J. Structures of a diverse set of colchicine binding site inhibitors in complex with tubulin provide a rationale for drug discovery. *FEBS J.* **2016,** *283*, 102-111. DOI: 10.1111/febs.13555.

59. Wang, Q.; Arnst, K. E.; Wang, Y.; Kumar, G.; Ma, D.; White, S. W.; Miller, D. D.; Li, W.; Li, W. Structure-Guided Design, Synthesis, and Biological Evaluation of (2-(1H-Indol-3-

yl)-1H-imidazol-4-yl)(3,4,5-trimethoxyphenyl) Methanone (ABI-231) Analogues Targeting the Colchicine Binding Site in Tubulin. *J. Med. Chem.* **2019,** *62*, 6734-6750. DOI: 10.1021/acs.jmedchem.9b00706.